

Thermal Analysis

Information for Users



24 User Com

Dear Customer,

We are delighted to inform you that METTLER TOLEDO has been awarded the coveted 2006 “R&D 100 Award” for the DSC823^e Differential Scanning Calorimeter with the new HSS7 MultiSTAR[®] high sensitivity DSC sensor in the category of Thermal Analyzers. The DSC823^e calorimeter was introduced in 2005 and has been a major success. The “R&D 100 Award” is awarded annually to the developers of new products that represent the greatest improvement in technology of that year. There are 16 categories awarded each year and this is the 44th year of the awards presentation.

According to the R&D Magazine, “winning an R&D 100 Award provides a mark of excellence known to industry, government and academia as proof that the product is one of the most innovative ideas of the year.”

Influence of absorbed moisture on the mechanical properties of Polyamide 6

Marco Zappa

Polymer samples have to be conditioned for several days in an atmosphere of defined relative humidity to obtain a uniform moisture content. The dependence of the glass transition temperature and the mechanical modulus on the moisture content of the sample is measured using dynamic mechanical analysis (DMA) in the shear mode. It was shown that no significant desorption of water occurs during a measurement and that measurement results are not affected by this.

Contents 2/2006

TA Tip

- | | |
|--|---|
| - Influence of absorbed moisture on the mechanical properties of Polyamide 6 | 1 |
|--|---|

New in our sales program

- | | |
|---|----|
| - Thermosets booklet | 6 |
| - Posters | 7 |
| - TGA-FTIR-MS Interface | 8 |
| - IntraCoolers | 8 |
| - Microscope hot-stage cooling system | 9 |
| - Certified reference materials for thermal analysis from LGC | 9 |
| - TA precision weights (0.2 g, 1 g and 5 g) | 10 |

Applications

- | | |
|---|----|
| - Evaluation and interpretation of peak temperatures of DSC curves. Part 2: Examples | 11 |
| - Curie temperature measurements on nanocrystalline iron-based mechanically alloyed materials | 16 |
| - Thermal characterization of food products | 18 |
| - Determination of the content of organic material in clay | 21 |

Dates

- | | |
|------------------------|----|
| - Exhibitions | 23 |
| - Courses and Seminars | 23 |

METTLER TOLEDO

Introduction

Water behaves as a plasticizer for many amorphous and semicrystalline plastics. Technically relevant mechanical material parameters such as the elastic modulus and the glass transition temperature vary quite significantly depending on the moisture content (water content) of a material. Examples of plastics that spontaneously absorb moisture (water) from their surroundings are hygroscopic epoxy resins, polyurethanes, ABS polymers, polycarbonates and all polyamide derivatives.

This article describes measurements of Polyamide 6 (Nylon 6) and shows

- how dynamic mechanical analysis can be used to determine the dependence of the elastic modulus and the glass transition temperature on the absorbed moisture content,
- how the equilibrium (maximum) moisture content and the moisture uptake rate can be determined at different relative humidity levels and temperatures, and
- what conclusions can be drawn for correct sample conditioning in a humid environment.

Sample material: Polyamide 6

Polyamide 6 samples (GoodFellow), 1 mm thick, 3 mm long and 3 mm wide, were used for all the DMA, TGA and sorp-

tion experiments. This sample geometry corresponds to that typically employed for these techniques. The samples were dried under vacuum (0.1 mbar) at 60 °C for 24 hours in order to obtain defined starting material. The loss of mass of samples through drying was determined by TGA and was found to be less than 0.1% up to 240 °C (melting range endset: 230 °C). The dry samples were sealed airtight and stored at 25 °C until use.

Sample conditioning in desiccators

Samples were conditioned in desiccators at different relative humidity levels in order to obtain samples of different well-defined moisture content. The relative humidity (RH) in the individual desiccators was established using supersaturated solutions of sodium chloride (75% RH), sodium bromide (58% RH), potassium carbonate (43% RH), potassium acetate (22% RH) and pure water (100% RH).

The relative humidity in each desiccator was monitored using a Hygropalm 2 humidity instrument from Rotronic AG, Switzerland. The measurement accuracy was better than $\pm 2\%$ RH over the course of the experiments (about 200 hours). The desiccators at 100% RH were kept at room temperature (25 °C) and in warming cabinets at 40 °C and 65 °C. The samples were placed on metal gauze in the desiccators to ensure that the entire surface area of the samples was exposed to the surrounding atmosphere.

The moisture (water) content, w_w , as a function of conditioning time is shown in Figure 1 for the different RH conditions. Here w_w is defined as:

$$w_w = \frac{m_w}{m_w + m_p}$$

where m_w is the mass of absorbed water and m_p the dry mass of the polymer. m_w was determined by measuring the change in mass change due to conditioning. Any surface water was removed from the samples with absorbent paper before they were weighed. The time needed for removing the sample from the desiccator, cooling, drying, weighing and returning the sample to the desiccator was less than two minutes for each sample.

At room temperature, the time for Polyamide 6 to reach the equilibrium (maximum) moisture content was more than 100 hours, independent of the relative humidity used. At 100% RH, the time to reach equilibrium could be reduced to 20 or 5 hours by increasing the conditioning temperature to 40 °C or 65 °C respectively.

Consequences of sorption behavior

- Samples must be conditioned in a defined atmosphere for about 200 hours to obtain samples with the maximum moisture content at a given RH and temperature, independent of the relative humidity. Even with much thinner samples or at much higher conditioning temperatures, over 5 hours are needed.
- If samples are conditioned in the measuring instrument to measure changes in material properties, sufficient time must be allowed for the sample to reach equilibrium with the surroundings at each stage of the experiment.
- If the complex kinetic process of moisture absorption is not complete, the moisture is not uniformly distributed within the sample. This means that the properties measured are those of inhomogeneous samples.

Conditioning to maximum moisture content

The samples used for the following measurements were all conditioned for 200 hours at the appropriate relative humidity in the various desiccators. The samples were then stored in hermetically sealed aluminum crucibles until they were needed for experiments.

The sorption behavior of various samples is summarized in Figure 2. This diagram shows the maximum moisture content, w_w, \max , of samples plotted as a function of relative humidity (RH).

The diagram shows that the sample material absorbs only a small amount of moisture ($w_w \leq 1\%$) in the range 0% to 50% RH. From 50% RH onward, w_w, \max increases significantly with increasing RH. For example at 50% RH, w_w, \max is about 1%. The glass transition temperature T_g is then about 27 °C (see Fig. 4).

Figure 1. Moisture absorption by Polyamide 6 showing the moisture content, w_w , as a function of time for different relative humidity levels and temperatures.

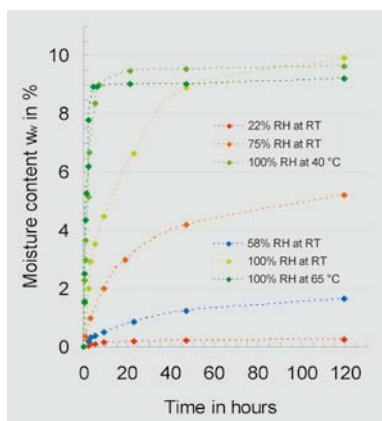
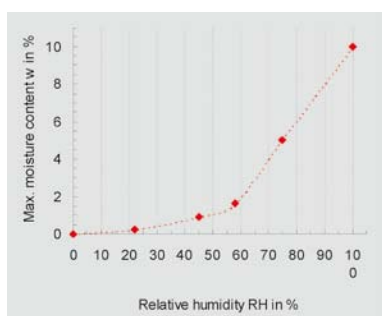


Figure 2. Sorption isotherm for Polyamide 6: The maximum moisture content, w_w, \max , plotted as a function of relative humidity RH (here shown for room temperature).



This value of T_g corresponds to the conditioning temperature (25 °C). From this it can be concluded that the maximum moisture content increases significantly when the surrounding temperature corresponds to the glass transition temperature. This can be explained by assuming that the increased free volume after the glass transition increases the moisture absorption of Polyamide 6.

$w_{w, \max}$ however shows only a slight temperature dependence. At 100% RH, $w_{w, \max}$ decreases by 1% between 25 °C and 65 °C (see Fig. 1).

Glass transitions of conditioned Polyamide 6 samples by DMA

The glass transitions of samples with moisture contents, w_w , ranging from 0 to 10.3% were measured in the DMA/SDTA861^e in the shear mode at 1 Hz using a heating rate of 3 K/min (see Fig. 3).

The glass transition temperatures were evaluated using the peak maximum of the loss modulus (G''), the peak maximum of the loss factor ($\tan \delta$) and the technically oriented determination according to DIN 65583 (the so-called 2% method) [1]. The values determined with the three methods for samples with moisture contents between 0% and 10.3% are summarized in Figure 4.

The shape of the glass transition temperature curve plotted as a function of the moisture content is practically independent of the evaluation method. The absolute values, however, differ systematically from one another according to definition. In the following discussion, the peak maximum of the loss modulus curve, G'' , is used to evaluate glass transition temperatures. Even small amounts of water ($w_w = 1.0\%$) cause the glass transition to shift from the original value of 62 °C in the dry state to about 30 °C. The glass transition temperature is around -25 °C for samples with the maximum moisture content. The greatest change in the glass transition temperature is observed from the dry state up to a moisture content of $w_w = 3\%$. From $w_w = 6\%$ onward, there is hardly any further change in the glass transition temperature.

In summary, it can be concluded that dry Polyamide 6 absorbs only a small amount of moisture ($w_w \cong 1.0\%$) up to

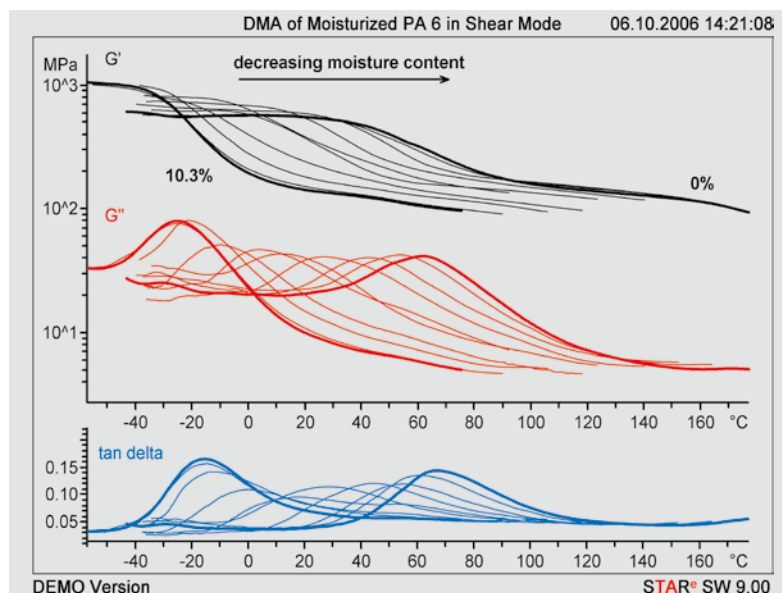


Figure 3. DMA measurements in the shear mode: Polyamide 6 samples with moisture contents, w_w , between 0 and 10.3%.

a relative humidity of about 50% (Fig. 2), but that this small amount causes a large decrease in the glass transition temperature (about 30 K, Fig. 4).

Desorption measured by TGA

The question arises of course as to whether desorption of moisture (water) during the measurement could influence the measurement results and in particular the value of the glass transition temperature, T_g . Loss of water below the melting point of water (0 °C) is difficult to imagine, so that an influence on the glass transition temperature is expected only when T_g (G'') is above 0 °C. According to Figure 4, this is the case at moisture contents of 0 to 4%. To determine how much water is lost on heating at 3 K/min, a series of samples was measured with the TGA/SDTA851^e (Fig. 5).

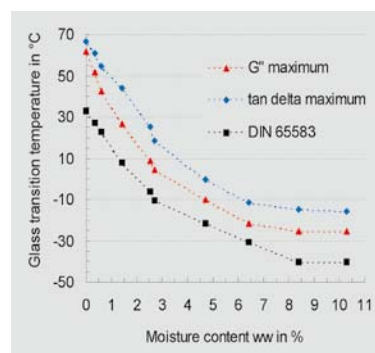


Figure 4. Glass transition temperatures of Polyamide 6 with moisture contents, w_w , between 0 and 10.3% measured by DMA in shear mode.

Since the influence of water loss on T_g is greatest for small water contents, samples with a moisture content of $w_w = 1.0\%$ (Fig. 5) were used for these measurements. At 3 K/min, a 10% reduction in moisture content was measured up until the end of the experiment at 60 °C. This corresponds to a mass loss of 0.1% relative to the total sample mass. This small amount represents the worst

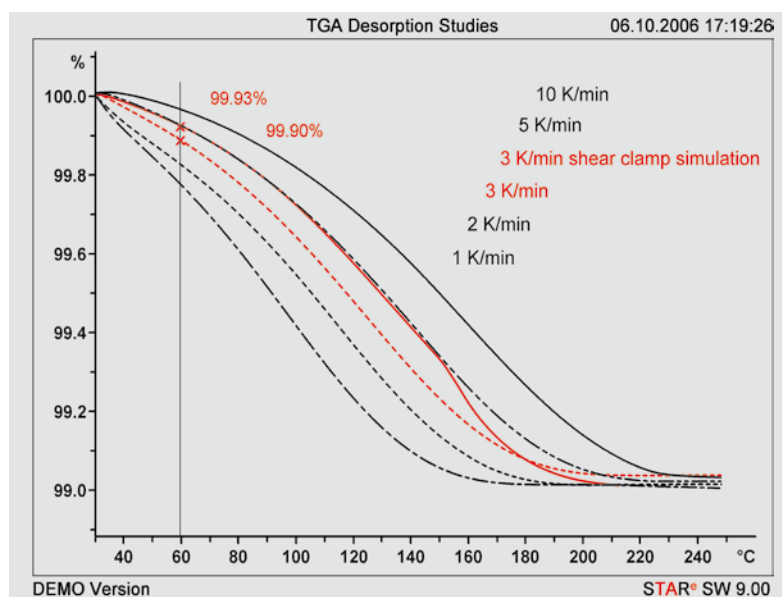


Figure 5. Loss of water from a Polyamide 6 sample with $w_w = 1.0\%$ measured at 3 K/min using the TGA/SDTA851^e.

possible case because in the TGA the entire surface of the sample is free for desorption to occur. In the DMA, however, the shear sample holder reduces the free sample surface area quite significantly so that a smaller water loss is to be expected. The shear sample holder effectively reduces desorption from the sample. This was confirmed in a further TGA experiment in which the surface area of a TGA sample was reduced to that of the free area of a sample in a DMA shear holder. Up to 60 °C, the mass loss corresponds to 7% of the moisture content or 0.07% relative to the sample mass. In Figure 5, this measurement curve is referred to as “3 K/min shear clamp simulation”).

Desorption during the DMA measurement in shear and bending

According to the previous section, the loss of water from the sample during a measurement is so small that no influence on the glass transition temperature is to be expected, or the error involved is within the measurement accuracy of the glass transition. This was confirmed by performing DMA measurements in shear

and bending (see Fig. 6). As long as the end temperature was below 70 °C, two successive measurements of the same sample showed no significant difference in the glass transition temperature. DMA measurements in shear mode have the advantage that the sample surface in contact with the surroundings is greatly reduced. But even 3-point bending measurements performed on samples (30 mm long, 10 mm wide, 1 mm thick) with a larger surface to volume ratio showed no significant differences in the glass transition temperature between two successive measurements of the same sample with $w_w = 1.0\%$.

This means that DMA samples do not have to be protected against loss of water during the measurement. Defined relative humidity as is sometimes used in the measuring cell during a measurement is obviously of no use here.

Silicone O-ring as water vapor barrier and immersion bath

Materials that react more sensitively to loss of water than Polyamide 6 or exhibit other desorption kinetics might possibly have to be protected against loss of water

- TGA measurements showed that the O-ring prevented desorption of water from the sample up to a temperature of 80 °C and that it can be used as a vapor barrier during measurements.
- No differences were observed in the glass transition temperatures when Polyamide 6 samples of different moisture content, w_w , were measured by DMA with and without silicone O-rings.
- The silicone rubber used for these experiments has a modulus of less than 10 MPa in the temperature range from -40 °C to +80 °C. If required, the absolute modulus values (G' and G'') of the sample can be obtained by subtracting the modulus value of the O-ring (using the geometry factor of the sample) from the modulus value of the sample measured with the O-ring (blank curve correction).

To follow changes in the elastic modulus as a function of time (isothermally), the silicone O-ring can also be used with the shear sample holder as an immersion bath for water or solvents. The advantages compared with traditional immersion baths are easy handling, external sample preparation, negligible thermal mass and accurate measurement of the sample temperature.

Elastic modulus and water content

Besides the glass transition temperature, the DMA measurements also allow the elastic modulus, G' , to be determined at different temperatures as a function of moisture content. This is shown in Figure 8 for temperatures of 0 °C, 25 °C and 40 °C.

Depending on the temperature considered, the elastic modulus decreases with increasing moisture content by a factor of three to four. The main reason for this decrease is that the glass transition temperature decreases with increasing moisture content. For 0 °C and 25 °C, however, the elastic modulus increases by 20% and 5% respectively between 0% and 1.5% moisture content. This stiffening of the material at low moisture contents is due to the fact that the modulus value in the glassy state increases linearly with increasing moisture content (see Fig. 9).

Figure 6. Comparison of the glass transition temperatures of Polyamide 6 measured by DMA ($\tan \delta$ maximum). The figure shows consecutive first and second heating runs measured at a heating rate of 3 K/min in shear and 3-point bending for samples with $w_w = 1.0\%$.

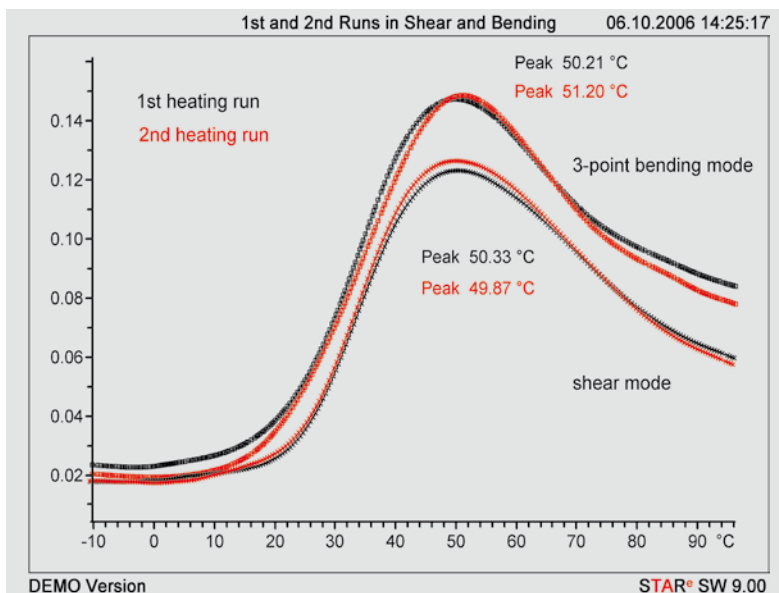


Figure 7. The shear sample holder with silicone O-ring as vapor barrier. TGA and DMA measurements showed that the O-ring was not needed for the DMA shear measurements of Polyamide 6.



during the measurement. In the shear mode, this was done by simply placing a silicone O-ring around the sample (see Fig. 7).

Experiments proved that the O-ring protects the sample against loss of water and at the same time does not introduce any measurement errors:

In the rubbery state after the glass transition, G' is in contrast practically independent of the moisture content. G' was determined at a temperature, T_p , with a defined difference of 60 K above the glass transition temperature, T_g (measured as the G'' peak maximum) i.e. such that $T_p = T_g + 60$ K.

Summary

Depending on the relative humidity, dry Polyamide 6 can absorb up to 10% by mass of moisture from its surroundings. This influences the glass transition temperature and elastic modulus of the material. The resulting effects were studied by first conditioning samples at different relative humidity levels (between 0 and 100%). This was done in desiccators containing different supersaturated salt-water systems. The maximum or equilibrium moisture absorption of a sample depends mainly on the relative humidity of the surroundings and to a lesser extent on temperature. Moisture absorption up to the maximum moisture content takes about 200 hours, independent of the particular relative humidity concerned. To exclude the possibility of measuring the properties of inhomogeneous samples, sufficient time must be allowed for the sample to attain its maximum moisture content before or during the measurement.

Dynamic mechanical analysis, DMA, of samples that had been conditioned to maximum moisture content shows that a moisture content of 1.0% lowers the glass transition temperature from 60 °C to 30 °C. The glass transition temperature of Polyamide 6 with the maximum possible moisture content (conditioning at 100% RH) is -25 °C. The elastic modulus of a sample with the maximum moisture content is about four times less than that of a sample in the dry state. In the glassy state, the material stiffens linearly with increasing moisture content and finally has a value twice that of the dry material. The modulus value after the glass transition is practically independent of moisture content.

Furthermore, TGA/SDTA851^e and DMA/SDTA861^e experiments showed that the loss of water from the sample during a measurement is so small that the measured values are not affected. Consecutive measurements of the same sample showed that the glass transition temperature did not change.

In conclusion, one can say that

- Samples must be conditioned at a defined relative humidity sufficiently long for the sample to attain a homogeneous distribution of moisture in the sample.
- In a DMA measurement, there is no need to protect the sample against loss of moisture. There is therefore no advantage in performing measurements under conditions of defined relative humidity in the measuring cell as is sometimes recommended.

Relative humidity

The relative humidity (RH) is the ratio, p/p_0 , of the water vapor pressure, p , (partial pressure) in a sample of moist air to the saturation water vapor pressure (p_0) at the same temperature expressed as a percentage. For example, at a relative humidity of 50%, air contains only half of the maximum amount of water vapor it could hold at that particular temperature. At 100% relative humidity, air holds as much water as it possibly can, i.e. it is fully saturated with water vapor (Fig. 10). If 100% saturation is exceeded, the excess moisture precipitates as condensation. The amount of water vapor needed to attain saturation increases with increasing temperature because the saturation water vapor pressure, p_0 , of air increases exponentially with temperature. For example, at normal pressure, a cubic meter of air at 10 °C can hold 9.41 g water. At 30 °C this value is already 30.38 g water. Since the maximum amount of water that air can take up changes with temperature, it is essential to state the temperature when quoting values of relative humidity.

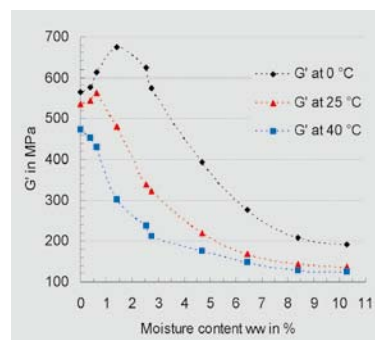


Figure 8. Elastic modulus, G' , of Polyamide 6 at 0 °C, 25 °C and 40 °C for samples of different moisture content, w_w .

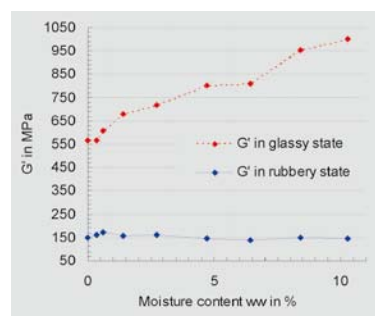


Figure 9. Elastic modulus, G' , of Polyamide 6 before and after the glass transition for samples of different moisture content, w_w .

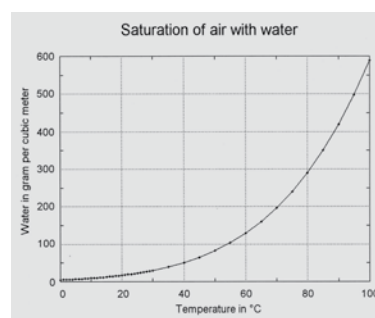


Figure 10. Maximum concentration of water in air at 100% RH for different temperatures.

Literature

- [1] The glass transition temperature measured by different TA techniques, UserCom 18, 1–5.

Thermosets booklet

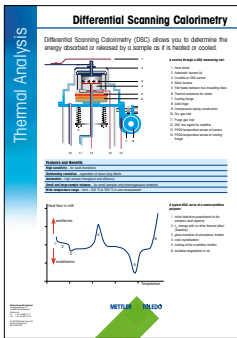
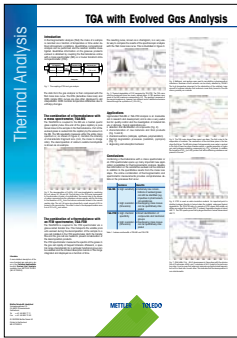
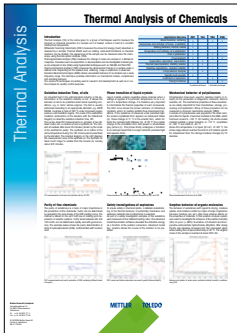
We are delighted to announce the availability of the new Thermosets Collected Applications booklet. This completes our very successful Collected Applications series. There is now a comprehensive collection of applications for practically every field of interest together with additional information for special areas.

Applications booklet	Language / Order number	Contents
New: Thermosets (300 pages)	English: 51 725 069 (Volumes 1 and 2) Volume 1: 51 725 067 Volume 2: 51 725 068	Thermosets comes in two volumes. It provides an insight into the thermal analysis (TA) of thermosetting materials and describes the results obtained from more than 90 practical examples. Volume 1 first presents a brief description of the various TA techniques used to analyze thermosetting materials. This is followed by an introduction to the chemistry and applications of thermosetting resins. The main part of Volume 1 discusses the properties and effects that can be investigated using, DSC, TGA, TMA and DMA. Volume 2 concentrates on practical examples and discusses the results obtained from more than 10 different types of resin including epoxies, polyesters, formaldehyde resins and polyurethanes. The applications describe the different properties that can be investigated, checked and measured during the lifecycle of a thermoset.
Thermoplastics (150 pages)	English: 51 725 002	Thermoplastics discusses the thermal behavior of more than 20 thermoplastics with the aid of some 59 application examples. Besides very many DSC, TGA and TMA experiments, 8 DMA examples are included in the latest edition. The effects investigated are: melting, crystallization, glass transition, softening, drying, thermal decomposition, oxidation stability, and expansion and contraction behavior. Practical questions such as thermogravimetric compositional analysis or how to avoid mistakes in the identification of materials are also dealt with. Dynamic mechanical analysis (DMA) is used to investigate the viscoelastic behavior of solids. Practical issues such as thermogravimetric content determination and how to avoid mistakes in the identification of materials are some of the important topics dealt with in the booklet.
Elastomers (275 pages)	English: 51 725 061 (Volumes 1 and 2) Volume 1: 51 725 057 Volume 2: 51 725 058	Elastomers comes in two volumes. It provides an insight into the thermal analysis (TA) of elastomers and describes the results obtained from over 50 practical examples using DSC, TGA, TMA, and DMA, as well as combined techniques for gas analysis (TGA-MS and TGA-FTIR). Volume 1 first presents a brief description of the various TA techniques used to analyze elastomers and is followed by an introduction to the chemistry and applications of elastomeric materials. The main part deals with the basic principles of thermal effects and their evaluation. Besides compositional analysis using TGA, the measurement of vulcanization and crystallization processes and the glass transition are also covered. Information on the optimization of measurement and evaluation techniques is also included. Volume 2 describes a large number of practical examples of elastomer analysis beginning with relatively simple examples through to analyses of complex systems and illustrates the different properties that can be investigated, checked and measured.
Pharmaceuticals (100 pages)	English: 51 725 006	Pharmaceuticals describes the application possibilities of thermal analysis in the pharmaceutical industry with the aid of 47 carefully selected examples. Melting behavior, polymorphism, purity, moisture as well as the stability of active and inactive ingredients are analyzed using DSC, TGA, EGA and TOA. The influence of measurement conditions and instrument calibration is also discussed.
Food (50 pages)	English: 51 725 004	Food demonstrates the application of thermal analysis to proteins, carbohydrates, fats and oils using some 53 DSC curves, 2 TGA curves and one TMA curve. The most important effects investigated are the: denaturation of proteins, swelling of starch in water, melting of sugar, thermal decomposition of sugar and starch, and the melting and crystallization of fats, oils and chocolate.

Evolved Gas Analysis (65 pages)	English: 51 725 056	Evolved Gas Analysis describes the combination of thermogravimetry (TGA) with gas analysis. The first part covers the basic principles of mass spectrometry (MS) and Fourier transform infrared spectroscopy (FTIR) as well as the interpretation of results and spectra. The practical part discusses 17 application examples using TGA-MS and TGA-FTIR techniques. Organic and inorganic samples as well as polymer systems are investigated. Besides the conventional TGA-MS and TGA-FTIR experiments, an example of an application performed with a TMA-MS combination is also described.
Tutorial Kit (25 pages)	Booklet German: 51 709 919 English: 51 709 920 French: 51 709 921 Booklet with test substances: German: 51 140 877 English: 51 140 878 French: 51 140 879	The Tutorial Kit booklet together with the corresponding test substances is excellent for self-study in thermal analysis. The power of thermal analysis is clearly demonstrated with 22 well-chosen examples.

Posters

METTLER TOLEDO has prepared a new series of posters covering the main TA techniques and areas of application. The posters are extremely useful for explaining the details of techniques and applications to visitors in your laboratory. The posters are available in A1 format (841 mm x 594 mm).

Poster type	Title	Number	Example
TA techniques	DSC	51 725 032	
	TGA/SDTA	51 725 035	
	TMA/SDTA	51 725 038	
	DMA/SDTA	51 724 319	
Conference posters	Temperature Modulated DSC	51 725 045	
	TGA-EGA	51 724 261	
Applications posters	Pharmaceuticals	51 725 046	
	Thermoplastics	51 725 047	
	Elastomers	51 724 320	
	Chemicals	51 724 461	

TGA-FTIR-MS Interface

Nowadays, one often wants to analyze the decomposition products evolved during a TGA measurement to gain a better understanding of the decomposition process. Usually either a mass spectrometer (MS) or Fourier transform infrared spectrometer (FTIR) is used. New is the possibility of measuring and analyzing the decomposition products

by MS and FTIR simultaneously. To do this the FTIR is coupled to the TGA instrument in the same way as before. The MS is then connected to the outlet of the FTIR using a new interface. Since the internal volume of the FTIR gas cell and transfer line is small, the time delay between the FTIR and MS measurements is negligible.



Figure 1. The TGA-FTIR-MS interface.

The advantages of this serial connection are:

- There is practically no contamination of the MS capillary
- The MS capillary cannot melt and seal (it is no longer exposed to the high temperatures in the TGA furnace)

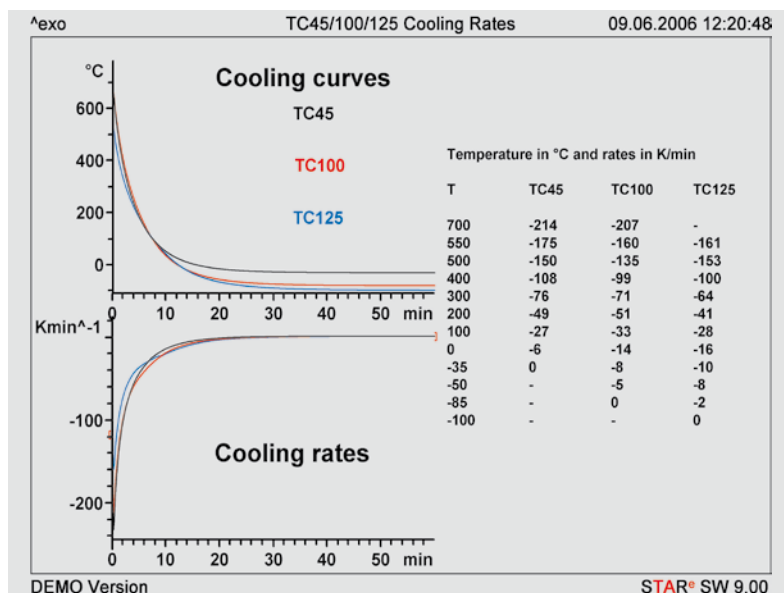
IntraCoolers

	Minimum temperature	Maximum temperature
TC45	-35 °C	700 °C
TC100	-85 °C	700 °C
TC125	-100 °C	550 °C

METTLER TOLEDO is now able to offer new IntraCoolers with a wider temperature range.

These new IntraCoolers are compatible with all DSC82x models.

Figure 1. Cooling rates of the three new IntraCoolers.



IntraCoolers are closed-circuit cooling systems and require practically no maintenance. The lower minimum temperatures result in faster cooling rates.

Microscope hot-stage cooling system

For the FP82HT and FP84HT microscope hot stage there is a new cold gas generator that allows measurements to be performed down to $-100\text{ }^{\circ}\text{C}$. The cold vapor needed for the microscope hot stage is

generated using a 50-L liquid nitrogen container through vaporization of liquid nitrogen on its outside wall. The microscope hot stage must be insulated to prevent icing.

Order Numbers:

Microscope hot-stage insulation:

ME 51 141 438

Cold gas generator:

ME 51 191 722

Certified reference materials for thermal analysis from LGC

Ben Joseph, LGC, United Kingdom

The LGC (Laboratory of the Government Chemist, UK) has a long history in the development and validation of analytical methods and the production of certified reference materials (CRMs) in support of these activities.

Through our distribution business, LGC Promochem, we provide a wide range of reference materials focused on a number of key market sectors including pharmaceutical testing, food analysis, environmental analysis, forensic science, clinical science and general analyte determination.

In the field of thermal analysis, LGC has produced a range of CRMs intended to help laboratories calibrate and check their thermoanalytical instruments. These materials have certified values for melting points, enthalpies of fusion and purity. Regular use of these CRMs gives the user confidence that his results are valid, reliable and traceable.

LGC is working to further improve thermal measurement facilities in the UK to secure the continuing supply of these reference materials. A new melting point facility, supported by the UK Department of Trade and Industry (DTI) through its Valid Analytical Measurement program is being commissioned and validated in collaboration with the UK's National Physical Laboratory (NPL).

In thermal analysis, the calibration and adjustment of analytical instruments is

crucial for the accuracy and reliability of measurement results. For example, the temperatures measured by thermoanalytical techniques such as differential scanning calorimetry (DSC), thermogravimetry (TGA), thermomechanical analysis (TMA) and dynamic mechanical analysis (DMA) must be correct. For quantitative DSC measurements, the heat flow also has to be calibrated and adjusted.

DSC is frequently used in the pharmaceutical industry for purity determination. In all cases, there is the urgent need for certified reference materials.

Melting point CRMs

LGC has produced a range of high purity organic melting point CRMs. Each material has a sharp melting point and is certified with respect to the onset of melting.

Material	Melting point ($^{\circ}\text{C}$)	Catalogue Number
Phenyl salicylate	41	LGC 2411
4-nitrotoluene	52	LGC 2401
Naphthalene	81	LGC 2402
Benzyl	95	LGC 2403
Acetanilide	115	LGC 2404
Benzoic acid	123	LGC 2405
Diphenylacetic acid	147	LGC 2406
Anisic acid	184	LGC 2407
2-chloroanthraquinone	210	LGC 2408
Carbazole	246	LGC 2409
Anthraquinone	285	LGC 2410

Table 1. Reference materials with certified melting points from LGC.

Material	Enthalpy of fusion (KJ/mol)	Catalogue Number
Indium	3.3	LGC 2601
Naphthalene	18.9	LGC 2603
Benzyl	23.3	LGC 2604
Acetanilide	21.8	LGC 2605
Benzoic acid	18.0	LGC 2606
Diphenylacetic acid	31.2	LGC 2607
Lead	4.8	LGC 2608
Tin	7.2	LGC 2609
Biphenyl	18.6	LGC 2610
Zinc	7.1	LGC 2611
Aluminum	10.8	LGC 2612

Table 2. Reference materials with certified enthalpies of fusion from LGC.

Enthalpy of fusion CRMs

LGC's reference materials have been rigorously certified for enthalpy of fusion and melting temperature using an adiabatic calorimeter.

Purity CRMs

To enable purity measurements made by DSC to be properly validated, LGC has

developed a set of DSC purity standards. The set consists of six 0.5 g units of biphenyl gravimetrically doped with different amounts of benzil.

All the CRMs mentioned in this article were prepared and maintained with the support of the UK's Department of Trade and Industry through its Valid Analytical

Measurement program. Visit www.vam.org.uk.

For further information please contact LGC Promochem, Europe's most comprehensive source of reference materials:

LGC Promochem

Tel: ++44 (0) 20 8943 8480

E-mail: askus@lgcpromochem.com

Web: www.lgcpromochem.com

LGC Promochem - Supporting Laboratory Standards

Material	Impurity (mole%)	Catalogue Number
Biphenyl	0.1	LGC 2013
	1.1	
	1.6	
	2.1	
	2.6	
	3.1	

Table 3.
Reinheit von zertifizierten Referenzmaterial.



Figure 1.
TA precision weights.



Figure 2.
Precision ring weights of the METTLER TOLEDO microbalance.



Figure 3.
Precision weight set 1 mg to 500 mg.

TA precision weights (0.2 g, 1 g and 5 g)

Precision weights for thermal analysis

METTLER TOLEDO offers a set of precision weights specially prepared for thermal analysis. The calibration of the TGA balance can now be automated using calibrated precision weights. The new 200-mg weight is designed so that it can be used with the automatic sample robot.

The two internal ring weights of the TGA microbalance allow automatic adjustment of the characteristic curve of the balance.

By means of the external weights, the calibration is traceable to the primary standard in Paris.

Ordering information:

Weight class E2: ME 11116761 with calibration certificate in a wooden case (0.2 g, 1 g, 5 g).

Precision weight set 1 mg to 500 mg

For the calibration and testing of microbalances in the weighing range of interest for thermal analysis, METTLER TOLEDO also offers a set that contains precision weights of 1 to 500 mg.

Ordering information:

Weight class E2: ME 00158801 with calibration certificate in a wooden case (1 to 500 mg).

Both weight sets consist of a wooden case, tweezers and the precision weights with the corresponding certificates.

Further weights and weight sets can be found in the METTLER TOLEDO weights brochure (English: 117 95 461, German: 117 95 460, French: 117 95 462).

Evaluation and interpretation of peak temperatures of DSC curves. Part 2: Examples

Dr. Jürgen Schawe

With the aid of practical examples, different approaches are shown for obtaining thermodynamically relevant temperatures or at least comparable characteristic temperatures from the measured peak temperatures of melting peaks. This is especially important for materials with wide melting ranges or for the determination of phase diagrams. Furthermore, it is shown how reorganization processes can be identified by means of peak evaluation. Finally special points are discussed concerning peaks that originate from other events such as chemical reactions, second order phase transitions, vaporization, and so on.

Introduction

In Part 1 of this series [1], the basic principles concerning the formation of peaks in DSC are discussed. It is shown that the peak temperature depends on the heating rate, the sample mass and the thermal contact between the sample and sensor (and thus on the crucible and the purge gas used). Besides this, different peak temperatures are obtained depending on whether the evaluation is performed using the sample temperature or the program temperature (in the STAR[®] terminology the reference temperature). Finally it was shown that in the melting process the peak temperature follows the equation

$$T_m = T_{m,0} + \sqrt{2 R \Delta h} \sqrt{m \beta} \quad (1)$$

Here, T_m is the peak temperature, $T_{m,0}$ is the peak temperature extrapolated to a

heating rate and mass of zero, R is the relevant thermal resistance, Δh is the specific enthalpy of fusion, m is the sample mass and β is the heating rate.

If the peak temperature is plotted against the square root of the product of the sample mass and heating rate, a straight line is obtained whose slope depends on the specific enthalpy of fusion and the thermal resistance. The ordinate intercept of the temperature axis is $T_{m,0}$. We call a diagram such as this an Illers diagram because Illers first derived equation (1) and experimentally verified its validity for polymer melts [2].

The extrapolated peak temperature, $T_{m,0}$, corresponds to the equilibrium melting temperature of the crystallites melting at the peak maximum.

Based on the discussions in reference [1], approaches for evaluating peak tempera-

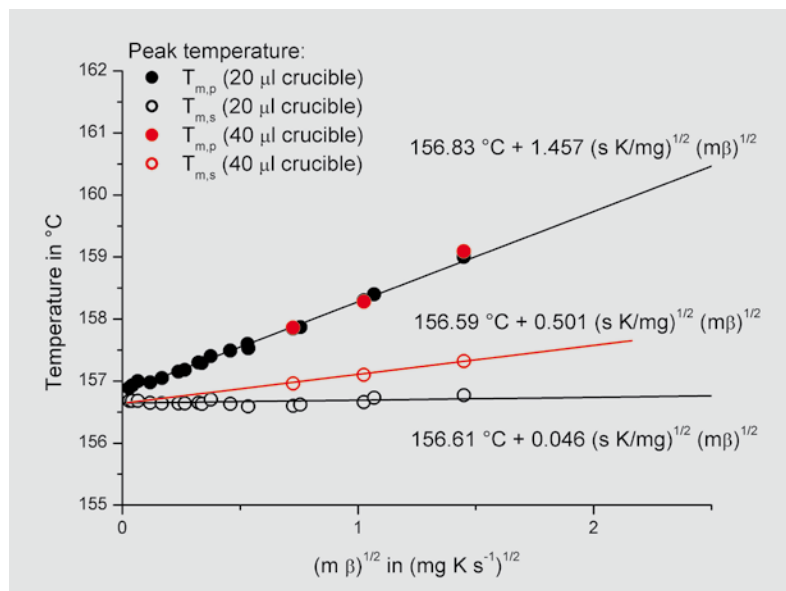
tures are discussed using practical examples. This deals mainly with melting processes but also refers to peak evaluation in other processes.

Melting of pure materials

The melting behavior of indium is used as an example to show the dependence of peak temperature on the experimental conditions. The melting temperature corresponds to the onset temperature of 156.6 °C. Four samples of different mass (0.053 mg, 0.846 mg, 3.425 mg and 6.301 mg) were measured at heating rates between 1 K/min and 20 K/min. The sample was enclosed in a light aluminum crucible (20 μ L; 21.9 mg aluminum). The program temperature, $T_{m,p}$, and the sample temperature, $T_{m,s}$, at the peak maximum were determined. Figure 1 shows the peak temperatures (black circles) in the Illers diagram. The results show that all the measurement points behave according to equation (1). The evaluation using sample temperature gives a much more gradual slope than that using the program temperature. The reason for this is the different thermal resistance relevant for the particular measurement. In the evaluation using the program temperature, it is the resistance between the sample and the furnace, R_f . In the case of the sample temperature, it is the resistance between the sample and the sensor, R_s .

To demonstrate the influence of the crucible, a sample (6.301 mg) was measured in a 40- μ L crucible (49.7 mg aluminum) at 5, 10 and 20 K/min. The corresponding peak temperatures are shown in Figure 1 as red circles. The sample temperature curves differ significantly depending on the type of crucible. The larger slope obtained with the 40- μ L crucible can be explained by the somewhat larger thermal resistance between sample and sensor. In the evaluation as a function of the program temperature, the difference

Figure 1. Illers diagram of indium measured in different crucibles. $T_{m,p}$ is the peak temperature evaluated as a function of the program temperature and $T_{m,s}$ is the corresponding sample temperature.



between these crucibles can be neglected because the thermal resistance between the sample and the furnace is many times larger.

The intercepts of the regression curves in Figure 1 yield the peak temperature extrapolated to a heating rate of zero. This should be the true melting temperature. As expected, it is 156.6 °C for both crucibles. The value is a little higher (156.8 °C) in the evaluation using the program temperature because the sample temperature was calibrated and not the program temperature. The temperature difference, ΔT , of 0.2 K corresponds to the difference between the sample temperature, T_s , and the program temperature, T_p [1].

These measurements show that the melting temperature can be determined from the peak temperature by extrapolating to a heating rate of zero in the Illers diagram. The evaluation should be performed using the sample temperature.

The melting peak in the case of metastable crystallites (polymers)

In contrast to the melting behavior of pure metals, the melting peaks of semi-crystalline polymers are often very broad. For this reason, an evaluation of the onset temperature does not provide representative and comparable values. The reason for the wide melting range has to do with the size distribution of the crys-

tallites. Small crystallites melt at a lower temperature than large, more perfect, crystallites. In general, the peak temperature is used to characterize the melting behavior. Analogous to the melting of pure metals, the peak temperature of these broad peaks depends on the sample mass and the heating rate. If materials are just being compared, measurements should be performed using samples of similar mass and at the same heating rate.

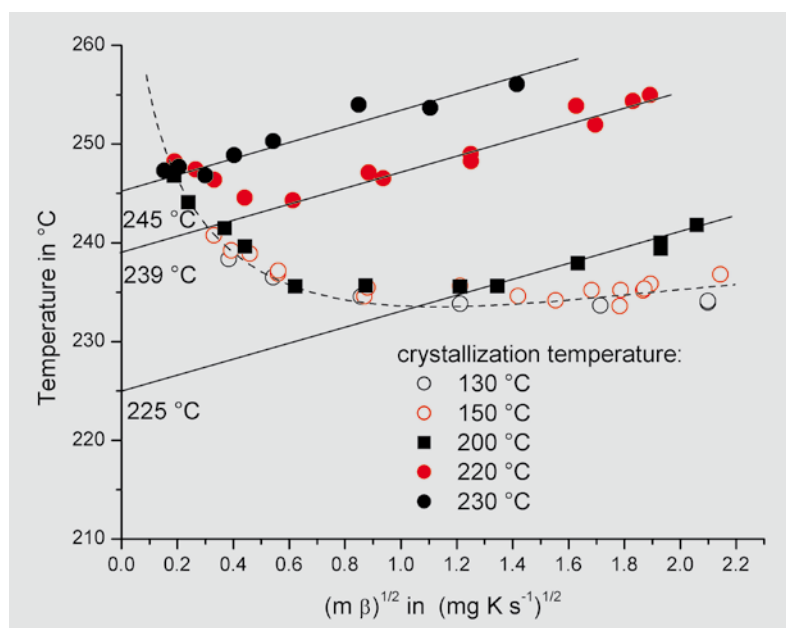
More information can be obtained if the measurements are performed at different heating rates. This is shown in the example of polyethylene terephthalate (PET). The equilibrium melting temperature of infinitely large crystallites in this polymer is about 280 °C. If the material is crystallized at temperatures between 160 °C and the equilibrium melting temperature, relatively large, stable crystallites are obtained. Below 160 °C, the crystallites are small and unstable. They melt on heating during the DSC measurement and can immediately recrystallize. Reorganization like this during the measurement shifts the melting peak to higher temperatures. This process cannot immediately be detected in a conventional DSC measurement because the enthalpies of melting and crystallization cancel each other out. To illustrate the influence of the different thermal stability of the crystallites on melting behavior, several PET samples were crystallized isothermally at 130 °C,

150 °C, 200 °C, 220 °C and 230 °C. The crystallization time was chosen so that it was ten times longer than the period between the beginning of crystallization and the maximum of the crystallization peak. Samples of mass between 0.5 and 3 mg were measured at heating rates in the range 1 to 400 K/min. The peak temperature of the main melting peak was determined using the sample temperature and plotted in an Illers diagram (Fig. 2).

The material crystallized at 230 °C has stable crystallites over the whole measurement range. The peak temperatures follow an Illers straight line. The ordinate intercept is 245 °C. This is the equilibrium melting temperature of the crystallites formed at 230 °C. If one looks at the peak temperatures of the samples crystallized at 220 °C, one sees that the peak temperature first decreases with increasing abscissa values but then, at about $0.6 \text{ (mg K s}^{-1}\text{)}^{1/2}$ (corresponding to a heating rate of about 20 K/min), follows a straight line. At the lower heating rates, the crystallites have sufficient time to recrystallize and to form larger crystallites. That is why the peak temperature lies above the corresponding Illers straight line.

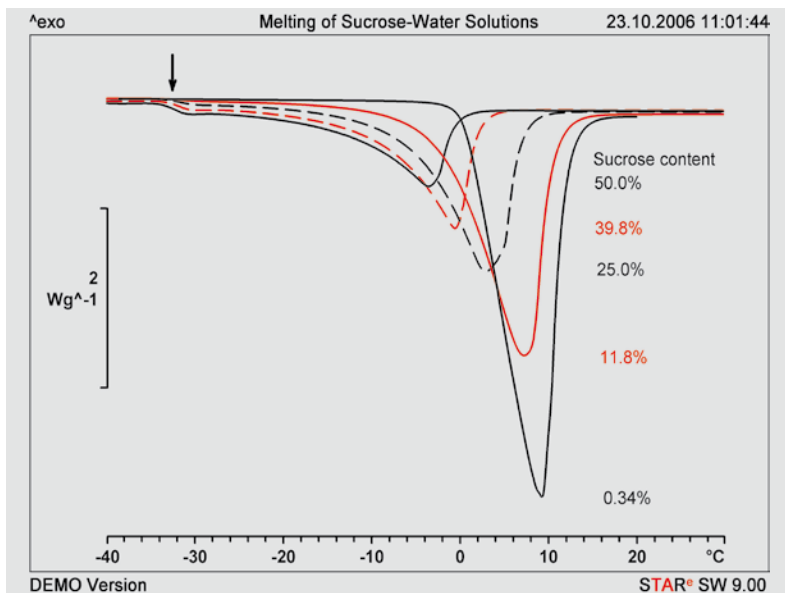
At heating rates above 20 K/min, the crystallites can no longer recrystallize during the measurement. The melting peak corresponds to that of the crystallites formed at the crystallization temperature of 220 °C. Their equilibrium melting temperature is 239 °C.

Figure 2. Illers diagram of samples of PET that had been crystallized at different isothermal temperatures. The continuous lines represent the melting behavior of stable crystallites. The dashed curve characterizes the curve for crystallites undergoing reorganization. The temperatures on the right side of the ordinate axis are the melting temperatures of the crystallites produced in the crystallization.



The samples crystallized at 200 °C behave similarly but the crystallites formed at this temperature are less stable. The region of reorganization is therefore larger. These crystallites can only be measured without recrystallization effects occurring when an abscissa value of $1.2 \text{ (mg K s}^{-1}\text{)}^{1/2}$ (i.e. about 100 K/min) is reached. The corresponding equilibrium melting temperature is 225 °C.

The samples crystallized at the lower temperatures exhibit reorganization over the entire measurement range. The peak temperatures follow the curve of the reorganized crystallites. The corresponding crystallites are also very unstable. Information about the stability of the crystallites of metastable materials can



therefore be obtained by evaluating the peak temperature.

The melting of multiphase systems (phase diagram)

In studies of multiphase systems, broad melting processes may occur whose measurement can be used to determine phase diagrams [3, 4]. The solidus line characterizes the beginning of the melting process, while the liquidus line determines the end of the melting processes. The beginning of the melting processes can often be determined directly with good accuracy from the DSC curves. In contrast, uncertainty can arise in the determination of the liquidus temperature, (end of melting).

The determination of the end of the melting is discussed using the system sucrose/water as an example. To do this, aqueous solutions with different sugar concentrations were prepared. Samples of mass between 16 and 23 mg were sealed in 40- μ L crucibles and cooled to $-100\text{ }^{\circ}\text{C}$ at 2 K/min. The samples were then measured at a heating rate of 5 K/min. Figure 3a shows typical curves of the melting region. The beginning of melting can be read off directly from the measurement curves. In Figure 3a this is marked by an arrow. The end of melting is close to the peak maximum. If one determines the peak maximum temperature (from the sample temperature), values are obtained that are too large (see Fig. 3b).

An accurate determination of the end of melting can be done using equation

(1) and the Illers diagram. This however requires at least four measurements at different heating rates for each measurement point. The end of melting is then the peak temperature extrapolated to a heating rate of zero.

A more rapid evaluation method that is slightly less accurate uses the difference between the onset and the peak temperature of the melting of the pure components. In this case, the melting of about 20 mg water is measured and the peak temperature, T_m , the onset temperature, T_{on} , and the heat flow at the peak maximum Φ_{max} are determined. These values are used to calculate a correction factor R_c :

$$R_c = \frac{T_m - T_{on}}{\Phi_{max}} \quad (2)$$

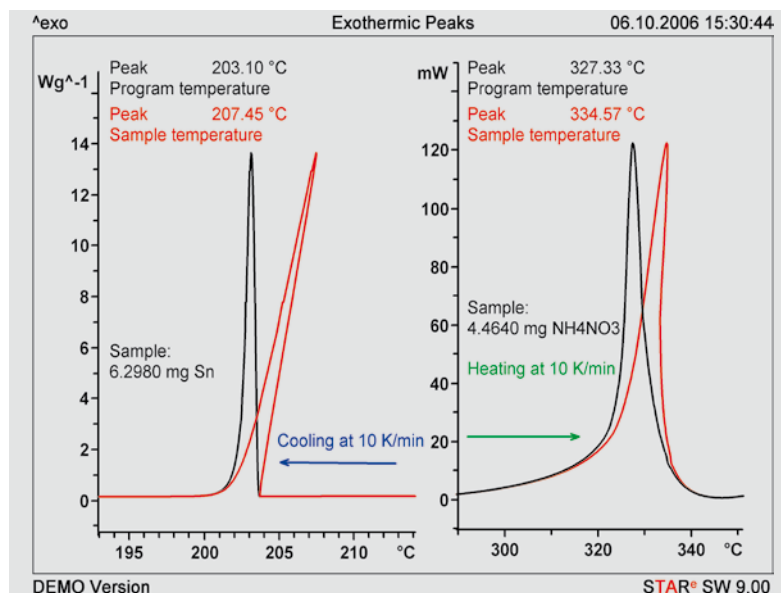
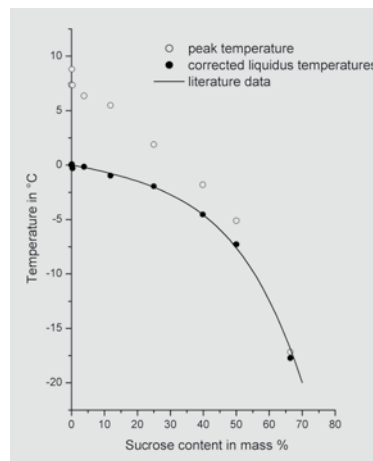


Figure 3. a) A series of melting peaks of sucrose/water mixtures of different concentration. The arrow marks the beginning of melting (concentration in mass %).

Figure 3. b) End of melting to determine the liquidus line.



The liquidus temperature, T_l , is obtained for each concentration from the corresponding peak temperature T_m by using the corresponding peak height, Φ_{max} :

$$T_l = T_m - R_c \Phi_{max} \quad (3)$$

Comparison of the literature data [5] with the values determined from the peak temperature using equation (3) shows acceptable agreement (Figure 3b).

Special points with other DSC peaks

Exothermic peaks

In endothermic processes, the heat flows from the furnace heater across the DSC sensor into the sample. In strongly exothermic processes, however, the direction of heat flow changes. The sample temperature in fact increases. This means that the sample temperature at the peak maximum is therefore higher than the corresponding program temperature. This is illustrated in Figure 4 which

Figure 4. Exothermic peaks measured from the crystallization of tin on cooling from the melt and the decomposition of NH_4NO_3 . The black curves are displayed using the program temperature and the red curves using the sample temperature.

shows the crystallization of tin on cooling from the melt and the decomposition reaction of NH_4NO_3 .

In the crystallization of tin, the curve of the sample temperature is linear from the beginning of crystallization at 203.5 °C to the peak maximum at 207.45 °C. The slope of this line is given by the thermal resistance between the sensor and the sample ($1/R_s$).

The difference between the program and sample temperatures becomes larger the higher the peak. The use of small samples and/or low heating rates is therefore recommended when large exothermic events occur. With exceptionally strong exothermic reactions, it may also be advisable to dilute the sample with an inert material (e.g. Al_2O_3). The increased heat

capacity then reduces the self-heating effect of the sample.

Chemical reactions

The peak temperature in a chemical reaction is largely determined by the kinetics of the reaction. For this reason, the Illers diagram cannot be used for the evaluation.

An optimum comparison of measurements at different heating rates (e.g. for obtaining information using reaction kinetics) should therefore be performed using small samples of similar mass (Fig. 5).

Second order phase transitions

With second order phase transitions, the heat capacity often increases up to a critical temperature. When this is exceeded, the heat capacity suddenly falls.

In DSC, this gives rise to an endothermic peak on heating (Fig. 6). Such transitions occur both with solid-solid transitions and with liquid-crystal transitions. The critical temperature is the peak temperature. With solids it can be influenced by the crystal size and internal stresses. Otherwise, the peak temperature is independent of the heating rate. In addition, in contrast to melting processes, the influence of heat transfer on the peak is small because the peaks are relatively small. In particular with liquid crystal transitions, the peak temperature is independent of the heating rate and does not exhibit supercooling. That is why these transitions are also recommended for the calibration of DSC instruments under cooling conditions [6].

The accuracy for the determination of the critical temperature increases at lower heating rates. To achieve maximum accuracy, the Illers diagram can be used with these peaks.

Vaporization peaks

Endothermic peaks occur during the vaporization of volatile components. The peaks are always coupled with a loss of mass from the sample (Fig. 7).

If free or weakly bound solvents are vaporized, the peaks are relatively broad. The situation is different when the volatile components escape in phase transitions (e.g. dehydration) or occur in chemical reactions (e.g. polycondensation). The loss of volatile components with corresponding peaks on the DSC curve is only observed if the measurement is performed in crucibles that are not hermetically sealed. In the evaluation of such processes, the mass of the sample is determined before and after the DSC measurement.

Besides this, repetition of the measurement using a variety of different crucibles such as completely sealed, with a 50- μm hole in the lid (self-generated atmosphere) or an open crucible (lid with large hole) is helpful. Since vaporization peaks often overlap other thermal events, the use of temperature-modulated DSC methods [7, 8] or a pressure DSC is recommended.

Figure 5. Example of the curing reaction of an epoxy resin-amine hardener system measured at different heating rates. The peak temperature (in K) is shown in the activation diagram ($\log \beta$ versus $1/T$). The slope of the straight line can be interpreted as the apparent activation energy.

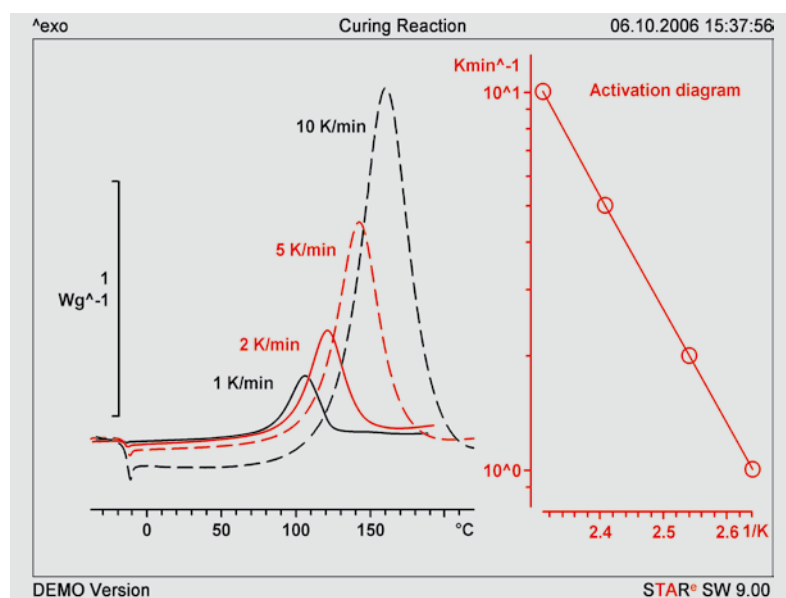
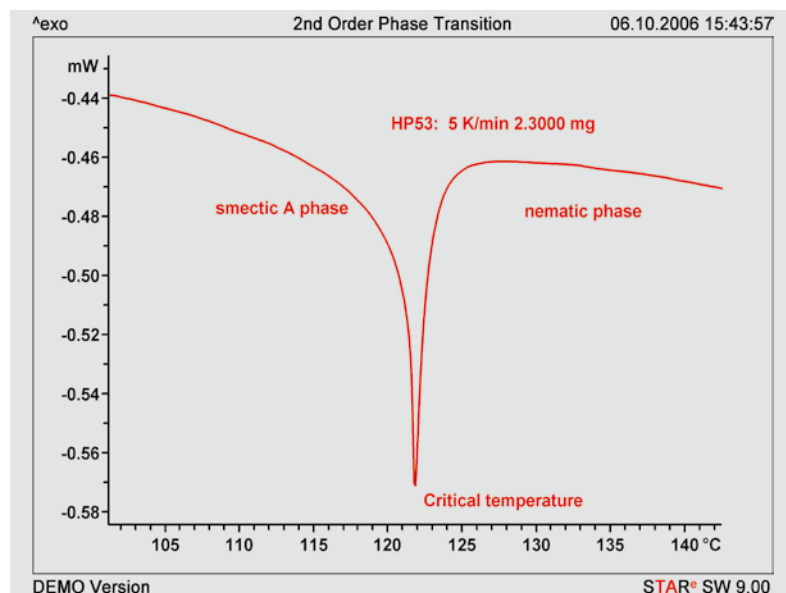


Figure 6. Example of a second order phase transition of a liquid crystalline material, in this case the transition from the smectic A phase to the nematic phase.



Enthalpy relaxation

In supercooled melts, the liquid specific cooperative molecular rearrangements become “frozen in”. A glass is formed. This glass is in a state of thermodynamic disequilibrium. The enthalpy of the glass is reduced through storage or mechanical stresses.

When a sample is heated, the effect induces a peak that overlaps the glass transition (Fig. 8). The temperature range of the enthalpy relaxation peak depends on the measurement conditions and the conditions of the enthalpy relaxation. An evaluation of the enthalpy relaxation should therefore always be performed in relation to the evaluation of the glass transition [9, 10].

The size of the enthalpy relaxation is determined by the integration of the difference between the curves (fresh sample, aged sample).

Conclusions

The peak temperature is an important quantity in the evaluation of thermal events in DSC. It is, however, influenced by the actual experimental conditions.

To interpret and determine characteristic data, one has to know which thermal event is responsible for the peak. The following rules are helpful for this:

- Determine the mass of the sample before and after the measurement.
- Measure the sample on heating, cooling and heating a second time.
- Possibly repeat the measurement in sealed (or pierced lid) crucibles.
- Repeat the measurement at a different heating rate.

If materials are to be compared using DSC measurements, the measurements must be performed at the same heating rate using a similar sample mass. Especially with polymers and polymorphic materials, melting behavior depends on thermal history such as cooling rate and storage conditions. These parameters must therefore also be taken into account in any comparison.

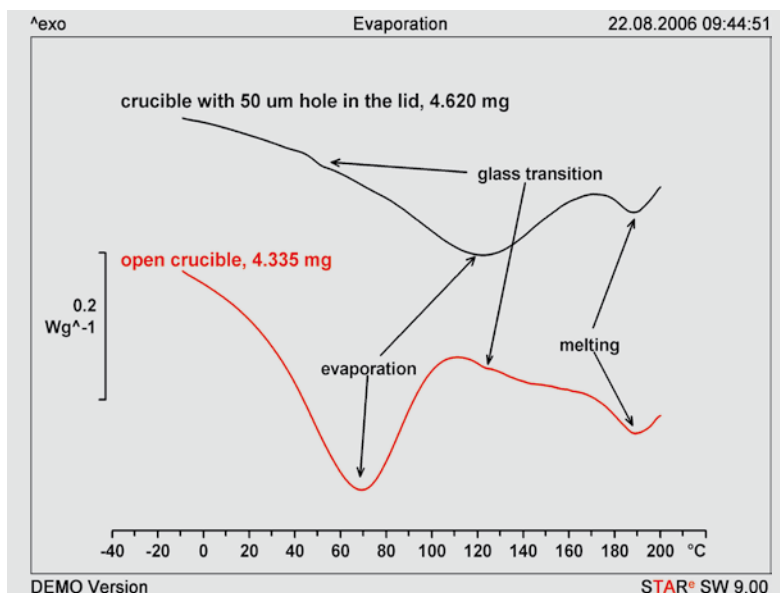


Figure 7. Hygroscopic polymer measured in an open crucible and in a crucible with a lid with a 50- μm hole. In the crucible with the small hole, a so-called self-generated atmosphere is formed. For this reason, the vaporization of the water is shifted to higher temperatures. The glass transition temperature is lower in the sample with the larger water content.

In general, peak temperature determination should be performed using the sample temperature. If the equilibrium temperatures in melting processes are required, the peak temperature must be measured using at least four different heating rates and the evaluation should be performed using the Illers diagram with extrapolation to a heating rate of zero. Information is then obtained about possible recrystallization processes during the measurement.

If a pure substance is available, the slope of the melting peak can be used to correct the measured peak temperature of melting processes of impure samples. Finally, the peak temperature can be de-

termined with better accuracy if small sample masses are used.

Literature

- [1] J. Schawe, UserCom 23, 6–9
- [2] K.-H. Illers, European Polymer Journal, 10 (1974) 911–916.
- [3] G. Widmann, UserCom 10, 18–19.
- [4] K. D. Beyer, UserCom 18, 9–12.
- [5] Z. Bubnik and P. Kadlec, in M. Mathlouthi and P. Reiser (Ed.), *Sucrose: Properties and Applications*, Blackie Academic & Professional, London, 1995, 101–125.
- [6] S. Neuenfeld and C. Schick, *Thermochimica Acta*, 446 (2006) 55–65.
- [7] J. Schawe, U. Hess, UserCom 16, 16–18.
- [8] J. Schawe, U. Hess, UserCom 22, 16–19.
- [9] J. Schawe, UserCom 10, 13–16.
- [10] J. Schawe, UserCom 11, 8–13.

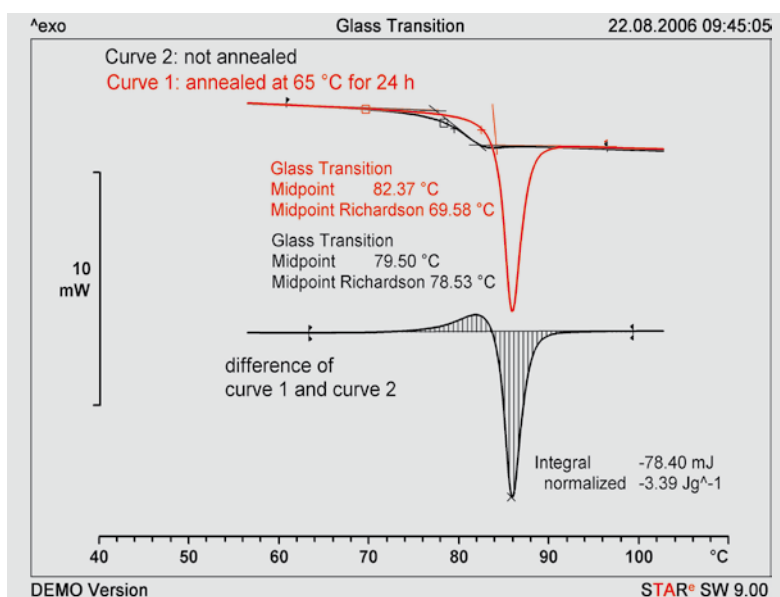


Figure 8. Glass transition of amorphous polyethylene terephthalate (PET) at a heating rate of 10 K/min. The annealed sample shows a marked enthalpy relaxation peak. This peak influences the evaluation of the glass transition (i.e. the glass transition temperature). The size of the enthalpy relaxation (3.39 J/g) can be determined from the integral of the difference between the two curves.

Curie temperature measurements on nanocrystalline iron-based mechanically alloyed materials

J.J. Suñol, A. Vilaró, GRMT, Dept. de Física, Universitat de Girona, Santaló s/n, 17071 Girona, Spain.
E-mail: joanjosep.sunyol@udg.es

Introduction

During the past decades, weakly magnetic materials such as amorphous Fe(Ni)-based alloys containing α -Fe nanocrystallites with the body-centered cubic (bcc) structure have been the subject of increasing interest. Their magnetic properties make them suitable for use in magnetic parts and devices such as low and high frequency transformers, alternating current machines, generators, induction coils, sensors and motors.

For such applications, it is important to determine the correct value of the Curie temperature (T_c) of materials, that is, the temperature at which the transition from ferromagnetic to paramagnetic behavior occurs. This characteristic temperature is often determined using thermoanalytical techniques [2].

This article describes how a METTLER TOLEDO TGA/SDTA851^e thermobalance was modified to measure the Curie temperature of materials by incorporating a small magnet.

Experimental details

The diagram in Figure 1 shows the two possible positions of the magnet. The upper position was chosen because it allowed the TGA to be used as a normal thermobalance and avoided potential problems with magnetic parts of the TGA. The magnet used had a field strength of about 10 mT (milliTesla). It was fixed in the same position for all measurements so that the magnetic field gradient acting on the sample was always the same. The first experiments were performed using high purity iron, cobalt and nickel stand-

ards to calibrate and adjust the TGA [3]. Mechanical alloying was carried out in a planetary ball mill (Fritsch Pulverisette P7) starting from pure elements (>99.5% purity) using a ball-to-powder mass ratio of 5:1. Oxidation was reduced by milling in an argon atmosphere. The milling process was performed at 600 rpm for 10, 20, 40 and 80 hours using stainless steel balls in a vial. The alloys produced were identified as Fe₈₀Nb₁₀B₁₀ (alloy A) and Fe₆₅Ni₂₀Nb₉B₆ (alloy B) using X-ray diffraction. The thermal behavior of the samples was followed using simultaneous DTA. Small amounts of the milled materials were annealed at 300 °C to allow structural relaxation/reordering to occur.

Results and discussion

The transition from ferromagnetic to paramagnetic behavior is observed in the so-called thermomagnetic curve, TM, as an apparent change in weight caused by the change in the magnetic properties of the sample.

Figure 2 shows the TM curve of alloy A, which had been milled for 10 hours. The first derivative of this curve, the DTM curve, was used to aid the evaluation. In magnetic measurements, the endset on the DTM curve is usually evaluated as the Curie temperature.

Sometimes the maximum of the DTM curve is used as the value of T_c . In Figure 2, the magnetic transition associated with iron was found to be 778 °C (endset). The slightly asymmetric shape of the DTM curve indicates inhomogeneity in the alloy. This is to be expected because the powder particles undergo severe mechanical deformation during mechanical alloying and are repeatedly cold-welded and fractured. It is therefore difficult to obtain homogeneous material using this technique. The minor event at 581 °C is attributed to the formation of a small

Figure 1. Schematic diagram of the TGA/SDTA851^e showing the two possible positions of the small magnet (red).

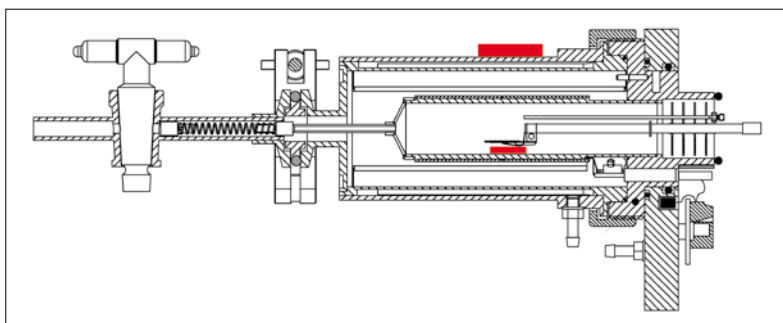
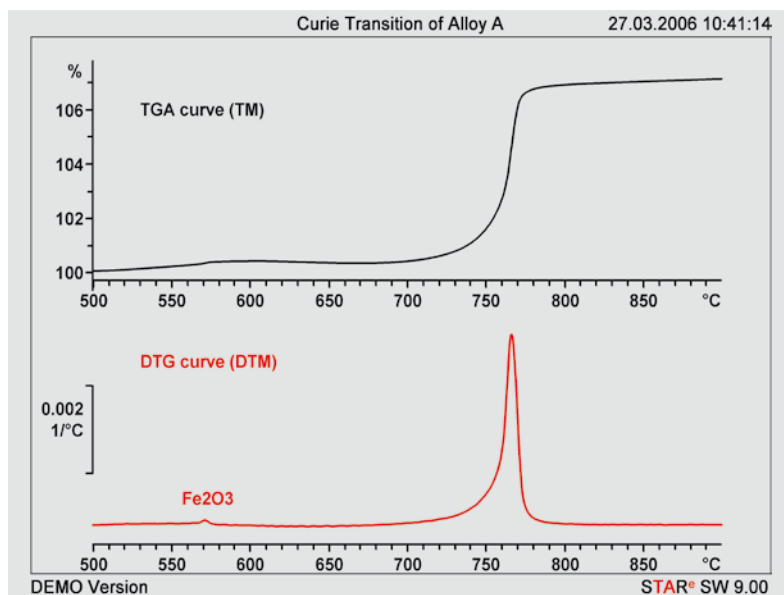


Figure 2. Thermomagnetic curve (TM) showing the apparent change in weight and the first derivative curve (DTM) for an Fe₈₀Nb₁₀B₁₀ alloy milled for 10 hours.



amount of iron oxide (Fe_2O_3) together with a larger magnetic effect. If necessary, this small oxidation effect (<1.0 atom % oxygen) can be eliminated by subtracting a curve of the same sample measured without the magnet.

The experiments performed with alloy B yielded results that are rather more complex. Figure 3 shows the curves measured after milling for 10 hours. The low temperature process at about 366 °C is associated with a face-centered cubic (fcc) Ni-rich phase.

The intermediate temperature process at 606 °C corresponds to a magnetic transition of an fcc (Ni, Fe) phase. The main process has an endset on the DTM curve at 769 °C and corresponds to the transition of an iron-rich phase. Both the asymmetric curve shape and the lowering of T_c are associated with the introduction of nickel by solid solution into the bcc iron. Figure 3 also displays the DTA curve. The thermal event beginning at about 200 °C is caused by structural relaxation or recovery from stress induced in the milling process. Several additional exothermic processes can be seen between 400 and 750 °C in the DTA curve. The temperature ranges of these processes overlap and correspond to the growth of crystallites that have been detected in alloys of similar composition by X-ray diffraction [4].

Table 1 shows the change of T_c as a function of milling time before and after and annealing at 300 °C.

In alloy A, without nickel, an increase in milling time lowers T_c only by about 10 to 20 K. Thermal treatment results only in very small changes. In alloy B, which contains nickel, several magnetic environments were found after milling for 10 hours. The nickel-rich low-temperature phase disappears after mill-

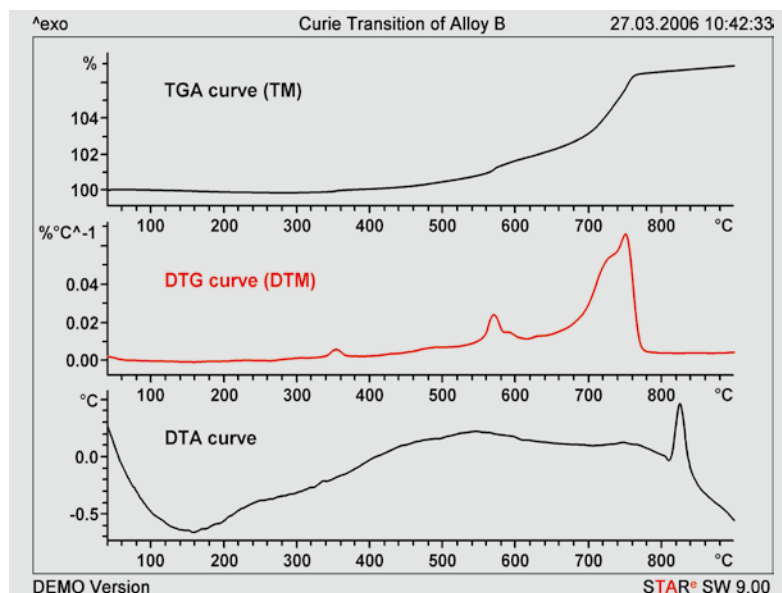


Figure 3. Thermomagnetic curve (TM) showing the apparent change in weight and the first derivative curve (DTM) for an $\text{Fe}_{65}\text{Ni}_{20}\text{Nb}_6\text{B}_9$ alloy milled for 10 hours.

Milling time	T_c alloy A in °C		T_c alloy B in °C	
	Milled	Milled and annealed	Milled	Milled and annealed
10 h	581	579	366	370
	778	776	606	601
			769	768
20 h	578	581	370	
	773	770	607	610
			765	745
40 h	582	577	603	604
	768	775	758	725
80 h	580	581	605	610
	752	772	742	

Table 1. Curie temperatures of alloys A and B milled or milled and annealed at 300 °C as a function of milling time.

ing for 20 hours. For these alloys, the low temperature phase disappears after milling for more than 10 hours. Finally, after milling for 80 hours, a homogeneous alloy was formed and just one T_c was observed.

Summary

A TGA/SDTA851^e thermobalance was modified with the aid of a small magnet (10 milliTesla) in order to determine the Curie temperature (T_c) of iron-based mechanically alloyed nanocrystalline alloys. The determination of the correct value of the Curie temperature is important because it provides information about the change from ferromagnetic to paramag-

netic behavior. The thermobalance was calibrated and adjusted beforehand using ferromagnetic elements (Fe, Co, Ni) as standards. Alloy formation can be followed as a function of time using TGA.

Literature

- [1] M.E. McHenry, M.A. Willard and D.E. Laughlin, *Progress in Materials Science* 44 (1999) 291–433.
- [2] G. Luciani, A. Constantini, F. Branda, P. Scardi and L. Lanotte, *J. Therm. Anal. Calorim.* 72 (2003) 105–111.
- [3] J.J. Suñol, A. González, L. Escoda, A. Vilaró, *J. Therm. Anal. Calorim.* 80 (2005) 257–261.
- [4] J.J. Suñol, T. Pradell, N. Clavaguera, M.T. Clavaguera-Mora, *Philosophical Magazine* 83-20 (2003) 2323–2342.

Thermal characterization of food products

Dr. Matthias Wagner

The thermal properties of a candy were completely characterized using “jelly bears” as an example. The glass transition temperature, composition, and the creep-, flow-, swelling- and frequency-behavior of two different commercial products were analyzed using differential scanning calorimetry (DSC), thermogravimetric analysis (TGA), thermomechanical analysis (TMA) and dynamic mechanical analysis (DMA).

Introduction

“Jelly bears”, the well-known German “Gummibären”, are similar to the English “jelly baby” sweets in appearance, taste and consistency.

They are ideal products with which to demonstrate the potential applications of thermal analysis in the food industry.

Between their production date and the time when they are finally eaten, jelly bears are exposed to widely different conditions such as temperature fluctuations, different frequencies, mechanical stress and different media.

These changing conditions can be simulated using thermal analysis instrumen-

tation and the properties of the product determined from the measurement results.

Jelly bears consist mainly of gelatin, a protein product, and different types of sugar. The carbohydrate content can be up to 78 percent by weight.

Due to the fact that the raw mass is obtained by heating the different ingredients and that the mechanical properties of the finished products contribute decisively to their enjoyment and taste, thermal analysis can provide an important contribution to maintaining constant quality and for the optimization of the production and the product properties.

Experimental details

Two different sorts of jelly bears manufactured in different countries were used as samples and are referred to as Sample A and Sample B. The samples were stored in a refrigerator prior to use. To eliminate the possible influence of different additives such as colorants, only red jelly bears were analyzed. The following thermal analysis instruments were used:

- DSC822^e with IntraCooler
- TGA/SDTA851^e
- TMA/SDTA841^e with automated liquid nitrogen cooling
- DMA/SDTA861^e.

Figure 1. DSC curves of two different sorts of jelly bears of different origin; one of the samples was measured fresh and also after drying. The effects that can be identified are the glass transition, drying, and decomposition.

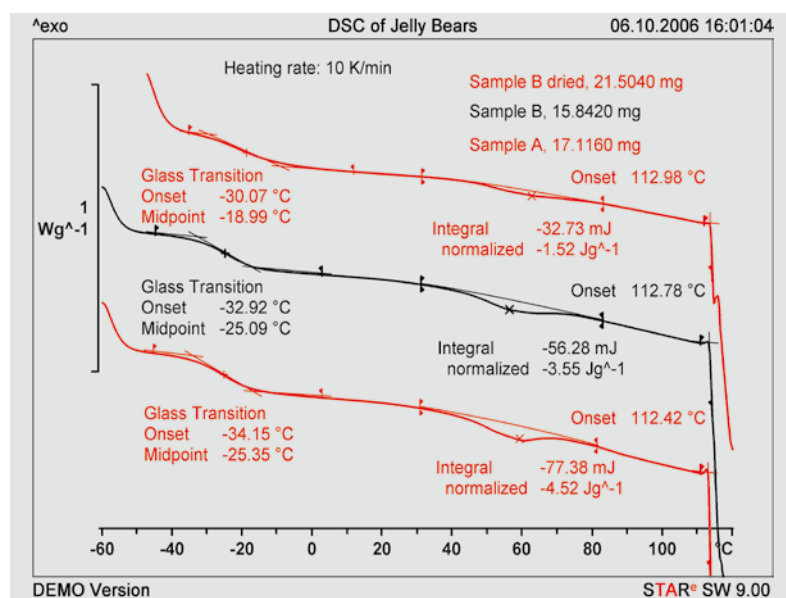
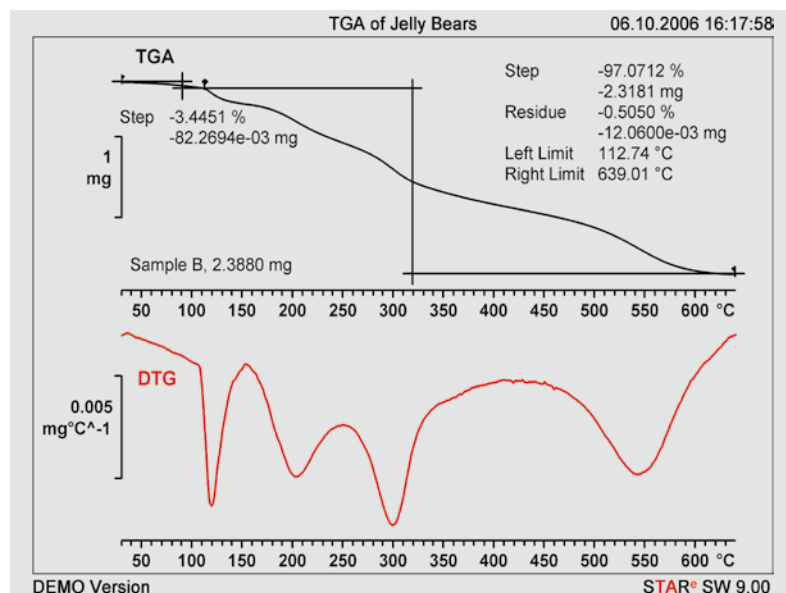


Figure 2. TGA and DTG curves of Sample B show the initial mass loss up to about 100 °C, which is probably due to the loss of moisture. The multi-step decomposition process begins at 112.7 °C.



DSC and TGA measurements were performed using 40- μ L aluminum crucibles with pierced lids. Small sample quantities were used for the TGA measurements because the samples tended to foam at the onset of decomposition.

Results

DSC

Figure 1 shows the DSC measurement curves of Samples A and B. One of the samples (Sample B) was also dried in air for half a day before measurement. All three curves showed a glass transition, a broad endothermic peak corresponding to the loss of moisture, and endothermic

behavior at the end of the measurement due to decomposition. The glass transition temperatures of the two fresh samples at about $-25\text{ }^{\circ}\text{C}$ differ only slightly. The moisture content of Sample A was about 25% higher than that of Sample B. This can be seen from the normalized integral of the peak area. All three samples decompose at about $112\text{ }^{\circ}\text{C}$. The moisture content of the dried sample is lower. This is apparent from the smaller normalized peak area and the higher glass transition temperature, T_g , of $-19\text{ }^{\circ}\text{C}$. Water acts as a plasticizer in this material, so the drier the sample, the higher the T_g .

TGA

The mass loss of Sample B as a function of temperature was measured by TGA (Fig. 2). The vaporization process below $100\text{ }^{\circ}\text{C}$ is followed by a multi-step decomposition process beginning at $112.7\text{ }^{\circ}\text{C}$. This value is in good agreement with the onset of decomposition determined by DSC.

TMA

The glass transition can also be measured by TMA. In this technique, the glass transition is observed as a change in the linear coefficient of expansion of the material as it changes from the glassy to the rubbery state. The characteristic glass transition temperature is evaluated as the point of intersection of the two tangents. Evaluation of the curves in Figure 3 yielded glass transition temperatures of $-29.7\text{ }^{\circ}\text{C}$ for Sample A and $-28.8\text{ }^{\circ}\text{C}$ for Sample B. The difference between the TMA temperatures and those determined by DSC is due to the fact that two very different measurement principles are used. Sample A expands more rapidly than Sample B.

Jelly bears are of course exposed to body fluids when they are eaten. These fluids can be both alkaline (saliva in the mouth) and acidic (gastric juices in the stomach). It is therefore interesting to study the swelling and dissolution behavior using TMA. In this case, this was demonstrated by exposing the samples to deionized water at room temperature. The resulting curves are shown in Figure 4. Sample A begins to swell immediately after the addition of the water. The ex-

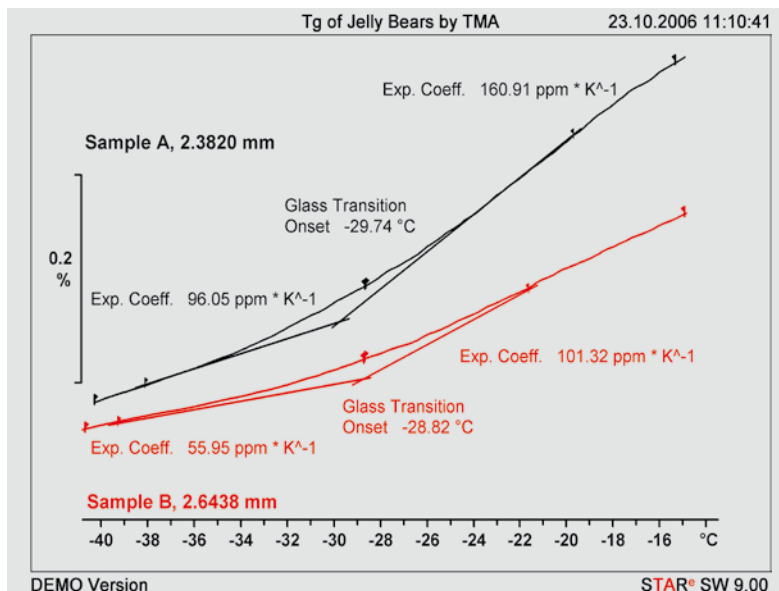


Figure 3. The glass transitions of jelly bears measured by TMA in the expansion mode.

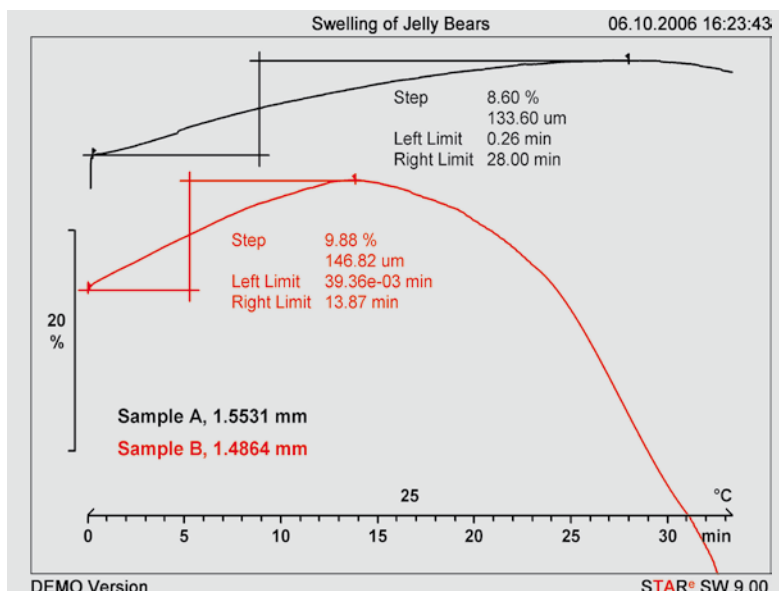


Figure 4. Isothermal swelling behavior in deionized water measured by TMA.

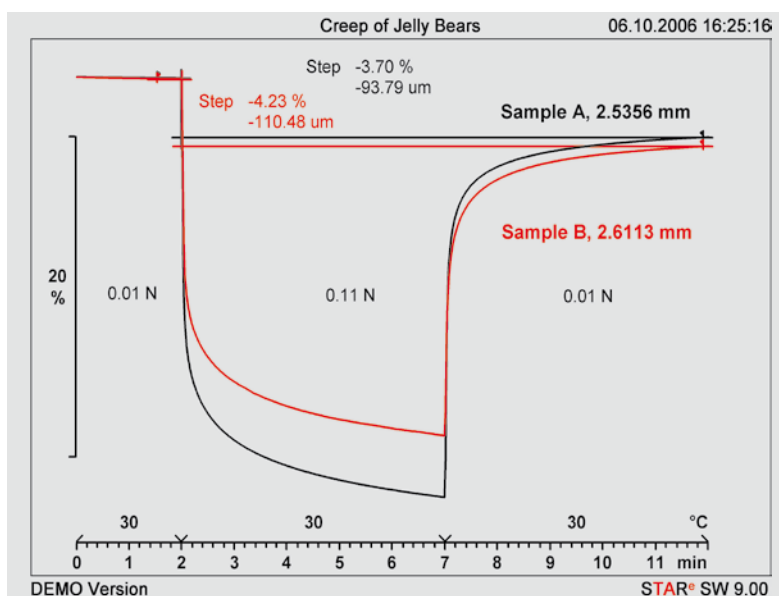


Figure 5. Creep experiments using TMA: Sample A yields significantly more under load, but recovers faster and more completely.

pansion is completed after 28 minutes and shows an 8.6% increase. The sample then begins to dissolve, which is seen as a

decrease in thickness. Sample B swells at a higher rate. The maximum expansion of 9.7% is reached after about 14 min-

utes. As before, the sample then begins to dissolve. The difference in swelling behavior of the samples has to do with the different processing conditions used during production, which results in a higher degree of crosslinking of the biopolymer in Sample A.

When the plastic bags containing jelly bears are packed into cartons, the jelly bears lower down are compressed by the weight of those lying above. This could lead to permanent deformation of the jelly bears, which would make them appear less appealing on the shelf in the shop.

This behavior (stress relaxation) of the elastomer-like material can be investigated using creep experiments. In such an experiment, a small force is first applied

to the sample, followed by a greater force for several minutes, and then the original small force again. The corresponding change in thickness and recovery time is continuously measured. Figure 5 shows such an experiment performed with both samples. Sample A yields significantly more under the applied force (i.e. it has a lower modulus) but recovers more rapidly and more completely, which is equivalent to it having higher creep resistance. Nevertheless, it has still not reached its original thickness even after 30 minutes.

The higher creep resistance confirms the result from the swelling experiment, namely that this sample is more strongly crosslinked. The lower value for the modulus is due to the higher content of water, which acts as a plasticizer.

DMA

During its product life cycle, a jelly bear is subjected to different frequencies, which correspond to different characteristic times. For example, the time spent in storage or lying on the shelf in the shop corresponds to a very long period (weeks), chewing to a short period (seconds) and shaking during transport by delivery truck over bad roads to a very short period (fractions of a second). The frequency-dependent mechanical behavior can be determined using dynamic mechanical analysis (DMA). The most suitable method for this is to use the Time-Temperature Superposition Principle (TTS).

Figure 6 shows the master curves obtained from Sample A from the evaluation of isothermal frequency scans in the shear mode. The storage and loss modulus at body temperature are shown as a function of frequency. One sees for example that the frequency range corresponding to chewing the material has a storage modulus of about 0.1 MPa, that is, it is viscous rather than elastic and so corresponds to the desired consistency for optimum chewing satisfaction.

Summary

Two different sorts of jelly bears were analyzed using four different thermal analysis techniques. DSC and TMA were used to determine glass transition temperatures. The values obtained depend on the moisture content. This can be determined using TGA and DSC, which also allow the onset of decomposition to be determined.

The most interesting results with respect to the end use (consumption) of jelly bears were obtained from the mechanical methods TMA and DMA. The swelling behavior in liquid media and creep behavior were determined by TMA, and the frequency-dependent behavior could be predicted from the DMA measurements. Table 1 summarizes the measurement results obtained with the four techniques.

Literature

[1] Thomas Lippert, Nachr. Chem. Tech. Lab., 1996, 44, 399–401

Figure 6. TTS experiment by DMA (shear mode). The diagram displays the storage modulus (black) and the loss modulus (red). The segments in the master curve determined for a reference temperature of 37 °C correspond to the shifted isothermal frequency scans.

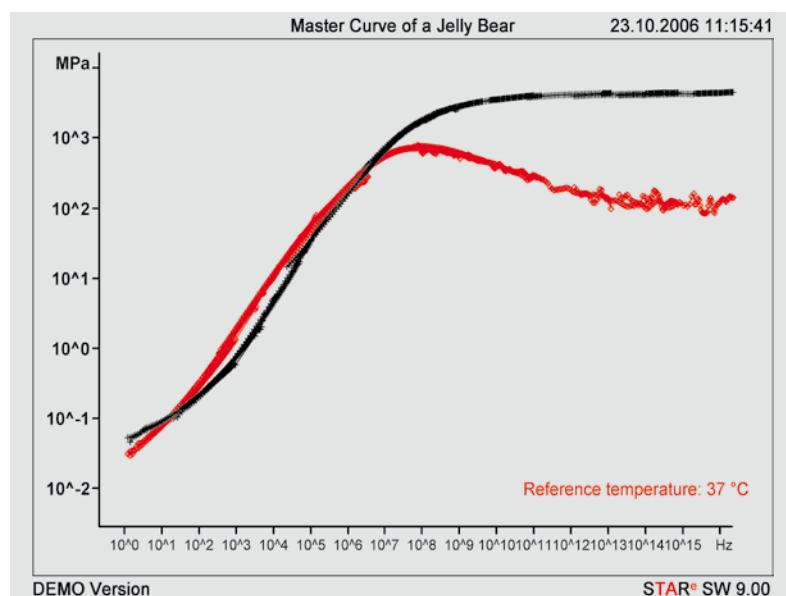


Table 1. Summary of the measured properties of Samples A and B.

Property	Sample A	Sample B	Technique
T_g in °C	-25	-25 fresh -19 dried	DSC
Moisture content in %	4.5	3.5 fresh 1.5 dried	DSC
Decomposition temperature in °C	112.4	112.8 fresh 113 dried	DSC
Moisture content in %	-	3.4	TGA
Decomposition temperature in °C	-	112.7	TGA
T_g in °C	-29.7	-28.8	TMA
Coefficient of expansion in ppm/°C	glass	96	TMA
	rubber	161	
Maximum degree of swelling in %	8.6	9.7	TMA
Swelling time to maximum in min	28	14	TMA
Creep resistance in %	3.7	4.2	TMA
Storage modulus, G' , at 37 °C / 1 Hz	0.1	-	DMA

Determination of the content of organic material in clay

Javier Pérez Martínez, Analyselabor Colorobbia España S.A.

This study looks at an analytical method for the determination of the content of organic material in clay using differential scanning calorimetry (DSC) and thermogravimetry (TGA). The results are compared with those obtained from the coulometric determination of the carbon content in the same samples.

Introduction

Clays are raw materials that are often used in different applications in ceramics and in the glass industry. In some of these applications, the content of organic materials in the clay is a factor that must be monitored because it influences the rheological properties and material behavior of the ceramic parts.

An accurate determination of the carbon content can be performed using a carbon analyzer. The sample is subjected to a combustion cycle and the liberated carbon is determined by coulometry.

In a thermal analysis experiment (Method 1) in which the clay is subjected to a combustion cycle of 25–1200 °C at a heating rate of 25 K/min in an air atmosphere, an mass loss is observed in some cases between 200 °C and 500 °C, which can be traced to the oxidation of organic substances (Fig. 1, Process 2).

In general, the end of the process coincides with the loss of water of crystallization of the clay minerals (Fig. 1, Process 3), which makes an accurate determination of the content of organic substances more difficult, especially with small amounts.

Experimental details

The measurements described here were performed using a TGA/SDTA851^e thermobalance. Care was taken to make sure that samples were as representative as possible. The sample material was homogenized before it was added to the crucible.

In view of the fact that a combustion process cannot occur in the absence of oxygen and that at 600 °C the water of

crystallization can be eliminated from most clay minerals, the optimized final method (Method 2) was:

1. isothermal at 25 °C for 10 min in nitrogen
2. heating to 600 °C at 10 K/min in nitrogen
3. isothermal at 600 °C for 20 min in nitrogen
4. isothermal at 600 °C for 15 min in air.

Results

The results obtained with this method can be seen in the TGA curves shown in Figure 2. This compares clay C, which contains organic material, with clay A, which contains none.

Clay C was chosen because it exhibits a low content of organic material. A car-

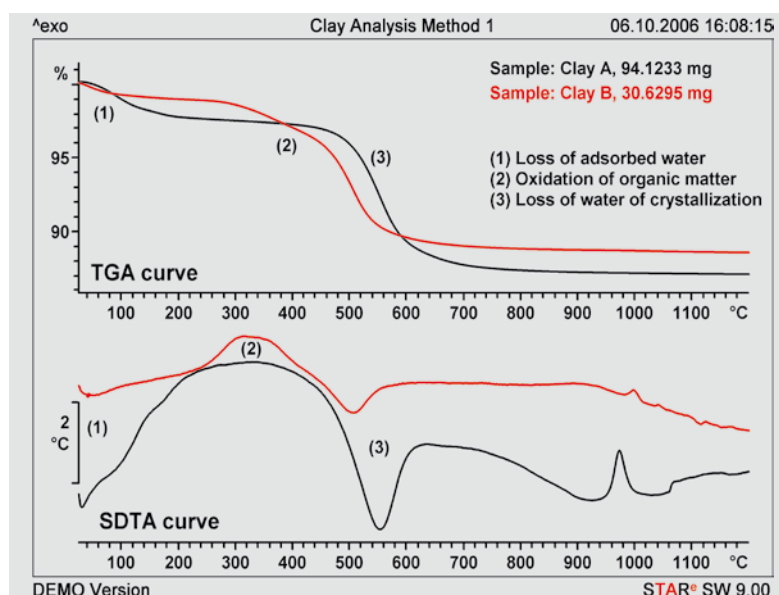


Figure 1. Properties of clay at a constant heating rate up to 1200 °C in an air atmosphere.

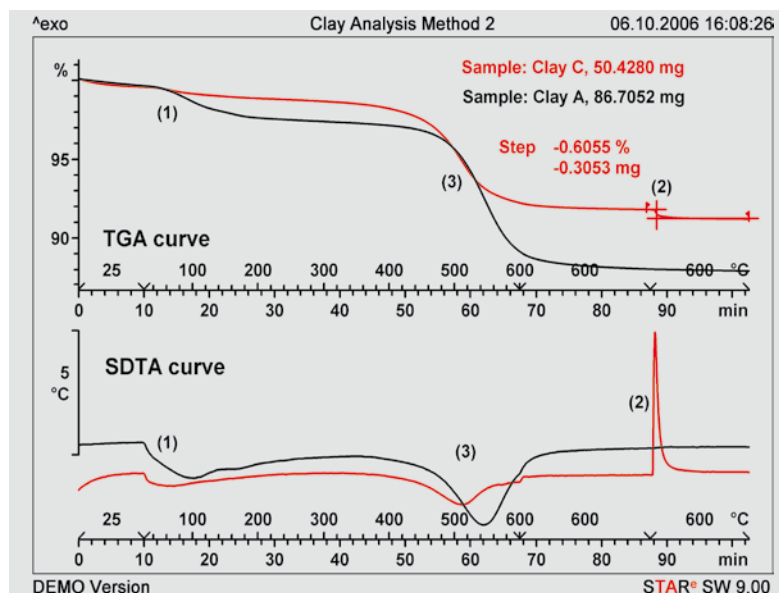


Figure 2. Stepwise loss of mass of clay using a method involving gas switching.

bon determination using coulometry was performed and the result compared with that obtained using differential thermal analysis (SDTA) and thermogravimetry (TGA) (see Table 1).

The results obtained from the measurements using thermal analysis, show only a small deviation (6.5%) from those from coulometry. This indicates that thermal analysis can be used for the reliable determination of carbon content.

The optimized method (Method 2) has the following advantages compared with the method shown in Figure 1 (Method 1):

1. The process of combustion of organic material (2) is separated from the other processes (1 and 3).
2. Clear TGA and SDTA signals are obtained by accelerating the combustion process.

Thermal analysis is used by Colorobbia España for the routine monitoring of clays. This allows small deviations to be

detected in the content of organic material within the same product lot and within different lots prepared over a period of time. Repeatability experiments performed using clay B yielded a content of organic mater of $0.90 \pm 0.02\%$.

The results presented in Figure 3 show the generally good repeatability of the method.

Conclusions

Both this study and values based on measurements of numerous industrial samples show that the results obtained with the TGA/SDTA 851^e using the method described above with gas switching are suitable for determining small differences in the content of organic material in clays.

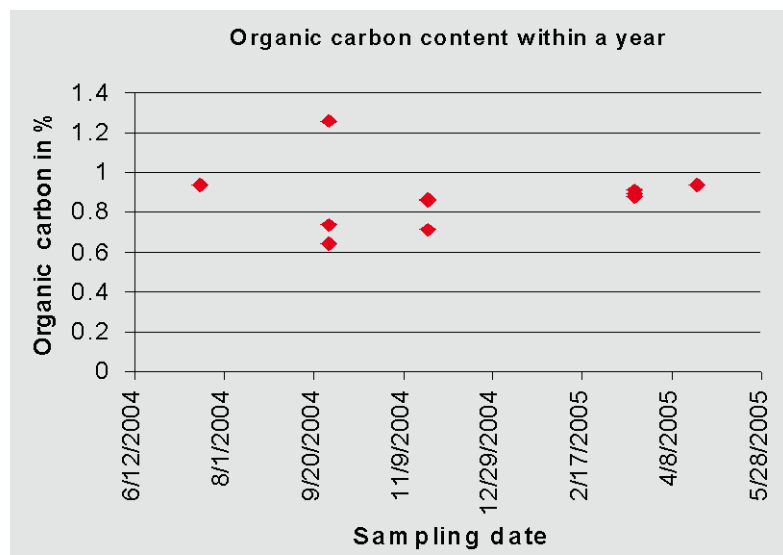
Literature

- [1] „Materias primas para la fabricación de soportes de baldosas cerámicas”, Instituto de Tecnología Cerámica (ITC) - AICE, 1997, Castellón, Spanien.
- [2] R. Riesen, UserCom 14, 18–20

Table 1.
Comparison of the determination of organic material by thermal analysis and by coulometry at 500 °C.

Sample	% Organic material	
	TGA/SDTA	Coulometry
Clay A	0	0
Clay C	0.61	0.65

Figure 3.
Measurement of deviations in the content of organic matter in clay in different product lots.



Exhibitions, Conferences and Seminars – Veranstaltungen, Konferenzen und Seminare

Pittsburgh Conference	February 26–March 1, 2007	Chicago, IL (USA)
Ulm-Freiburger Kalorimetrietage	March 21–23, 2007	Freiberg (Germany)
Analytical Sciences: Industrial Problem Solving	May 16–18, 2007	Newark, NJ (USA)
12 th International Congress on the Chemistry of Cement	July 8–13, 2007	Montreal, Canada
Federated Society for Coatings, Coating woods and Wood Composites for Durability Symposium	July 23–25, 2007	Seattle, WA (USA)
NATAS 2007	August 26–29, 2007	State University, Lansing, MI (USA)
ILMAC 2007	September 25–28, 2007	Basel (Switzerland)
K 2007	October 24–31, 2007	Düsseldorf (Germany)

International and Swiss TA Customer Courses:

TA Customer Courses and Seminars in Switzerland – Information and Course Registration:

TA-Kundenkurse und Seminare in der Schweiz – Auskunft und Anmeldung bei:

Frau Esther Andreato, Mettler-Toledo AG, Analytical, Schwerzenbach,
Tel: ++41 44 806 73 57, Fax: ++41 44 806 72 60, e-mail: esther.andreato@mt.com

Courses / Kurse

SW Basic (Deutsch)	12. Feb. 2007	17. Sep. 2007	SW Basic (English)	Feb 19, 2007	Sep 24, 2007
TMA (Deutsch)	12. Feb. 2007	17. Sep. 2007	TMA (English)	Feb 19, 2007	Sep 24, 2007
DMA Basic (Deutsch)	12. Feb. 2007	17. Sep. 2007	DMA Basic (English)	Feb 19, 2007	Sep 24, 2007
DMA Advanced (Deutsch)	13. Feb. 2007	18. Sep. 2007	DMA Advanced (English)	Feb 20, 2007	Sep 25, 2007
TGA (Deutsch)	13. Feb. 2007	18. Sep. 2007	TGA (English)	Feb 20, 2007	Sep 25, 2007
TGA-MS (Deutsch)	14. Feb. 2007	19. Sep. 2007	TGA-MS (English)	Feb 21, 2007	Sep 26, 2007
DSC Basic (Deutsch)	14. Feb. 2007	19. Sep. 2007	DSC Basic (English)	Feb 21, 2007	Sep 26, 2007
DSC Advanced (Deutsch)	15. Feb. 2007	20. Sep. 2007	DSC Advanced (English)	Feb 22, 2007	Sep 27, 2007
TGA-FTIR (Deutsch)	15. Feb. 2007	20. Sep. 2007	TGA-FTIR (English)	Feb 22, 2007	Sep 27, 2007
SW Advanced (Deutsch)	16. Feb. 2007	21. Sep. 2007	SW Advanced (English)	Feb 23, 2007	Sep 28, 2007

Local TA Customer Courses:

TA-Kundenkurse und Seminare in Deutschland

Für nähere Informationen wenden Sie sich bitte an: Frau Petra Fehl, Mettler-Toledo GmbH, Giessen,
Tel: ++49 641 507 404, e-mail: petra.fehl@mt.com

Anwenderworkshop DSC	06./07.03.2007	Giessen	04./05.09.2007	Giessen
Anwenderworkshop TGA	08./09.03.2007	Giessen		
Thermische Analyse und Rheologie in Forschung und Qualitätssicherung – Eine gemeinsame Veranstaltung der Unternehmen Thermo Electron und METTLER TOLEDO	13.02.2007	Hannover	28.03.2007	Wien
	20.03.2007	Potsdam	08.05.2007	Düsseldorf
			auf Anfrage: Zürich, Basel	

Cours et séminaires d'Analyse Thermique en France

Renseignements et inscriptions par: Christine Fauvarque, Mettler-Toledo S.A., 18-20 Av. de la pépinière,
78222 Viroflay Cedex, Tél: ++33 1 3097 1439, Fax: ++33 1 3097 1660

Principe de la TMA/DMA	1 octobre 2007	Viroflay (France)	Principe de la TGA	4 octobre 2007	Viroflay (France)
Principe de la DSC : les bases	2 octobre 2007	Viroflay (France)	Logiciel STAR® : perfectionnem.	5 octobre 2007	Viroflay (France)
Principe de la DSC : perfectionnem.	3 octobre 2007	Viroflay (France)			

Corsi e Seminari di Analisi Termica in Italia

Per ulteriori informazioni Vi preghiamo di contattare: Simona Ferrari, Mettler-Toledo S.p.A., Novate Milanese,
Tel: ++39 02 333 321, Fax: ++39 02 356 2973, e-mail: simona.ferrari@mt.com

DSC base	6 Febbraio 2007	12 Giugno 2007	25 Settembre 2007	Novate Milanese
DSC avanzato	7 Febbraio 2007	13 Giugno 2007	26 Settembre 2007	Novate Milanese
TGA	8 Febbraio 2007	14 Giugno 2007	27 Settembre 2007	Novate Milanese
TMA	9 Febbraio 2007	15 Giugno 2007	28 Settembre 2007	Novate Milanese
La corretta interpretazione dei tracciati termooanalitici			13 Marzo 2007	Milano
L'Analisi Termica nel Controllo Qualità e nella Ricerca e Sviluppo			22 Marzo 2007	Roma
			20 Marzo 2007	Napoli
			29 Marzo 2007	Padova

Cursos y Seminarios de TA en España

Para detalles acerca de los cursos y seminarios, por favor, contacte con: Francesc Catala, Mettler-Toledo S.A.E., Tel: ++34 93 223 76 00, e-mail: francesc.catala@mt.com

Aplicaciones del Análisis Térmico	Febrero, 13 de 2007	Zaragoza
	Septiembre, 25 de 2007	Barcelona
	Octubre, 2 de 2007	Madrid
Uso del sistema STAR [®]	Septiembre, 26 de 2007	Barcelona
	Octubre, 3 de 2007	Madrid

TA-Seminare in Österreich

Für nähere Informationen wenden Sie sich bitte an: Frau Geraldine Braun, Mettler-Toledo GmbH, Wien, Tel: ++43 1 604 19 80 - 33DW, e-mail: geraldine.braun@mt.com

Thermische Analyse und Rheologie in

Forschung und Qualitätssicherung 28. März 2007 Wien

TA Customer Courses and Seminars in the UK

For details of training courses and seminars, please contact: Rod Bottom, Mettler-Toledo Ltd, Leicester, Tel: ++44 116 234 5025, Fax: ++44 116 236 5500, e-mail: rod.bottom@mt.com

DSC BASIC	February 27, 2007	October 25, 2007	Leicester
-----------	-------------------	------------------	-----------

TA Customer Courses and Seminars in Singapore

For details of training courses and seminars, please contact: Bryan Yiew, Mettler-Toledo (S) Pte Ltd, 28 Ayer Rajah Crescent, #05 - 01, Singapore 139959 Tel: +65-68900011, Fax: +65-68900012, e-mail: bryan.yiew@mt.com

STAR [®] Infoday Seminar	April 2007	Singapore	
DSC BASIC	August 2007	November 2007	Singapore

TA School and Seminars in Korea

For details of training courses and seminars, please contact: KiHun Lee at Mettler-Toledo Korea, Tel: ++82 2 3498 3500, e-mail: kihun.lee@mt.com, Homepage: www.kr.mt.com

TA School for MT Users	April 2007	Seoul and DaeJeon
TA Public Seminar in 2007	October 2007	Seoul and Ulsan

TA Customer Courses and Seminars in China

For details of training courses and seminars, please contact: Lu LiMing at Mettler-Toledo Instruments (Shanghai) Co., Ltd., Tel: ++86 21 6485 0435, Fax: ++86 21 6485 3351, or by e-mail: liming.lu@mt.com

STAR [®] Customer Seminar	March 2007	Hangzhou
	April 2007	Hefei and Tianjin
	May 2007	Guangzhou and Kunming

TA Seminars in Japan

For details of seminars, please contact: Tomoko Wakabayashi, Mettler-Toledo KK, 3-8 Sanbancho, Chiyoda-ku, Tokyo 102-0075, Japan, Tel : +81-3-3222-7164, Fax : +82-3-3222-7124, e-mail: tomoko.wakabayashi@mt.com

STAR [®] Infoday Seminar	April 2007	Tokyo and Osaka
-----------------------------------	------------	-----------------

Editorial team



Dr. J. Schawe
Physicist



Dr. R. Riesen
Chem. Engineer



J. Widmann
Chem. Engineer



Dr. M. Schubnell
Physicist



Dr. M. Wagner
Chemist



Dr. D. P. May
Chemist



Ni Jing
Chemist



Marco Zappa
Material Scientist



Urs Jörimann
Electr. Engineer

Mettler-Toledo AG, Analytical

Postfach, CH-8603 Schwerzenbach

Phone ++41 44 806 73 87

Fax ++41 44 806 72 60

Contact: urs.joerimann@mt.com

www.mt.com/ta

For more information